y No. 59

Copy #1

AMP Report 42. 1R
AMG-NYU No. 105

NEW YORK UNIVERSITY
INSTITUTE OF MATHEMATICAL SCIENCES
LIBRARY
25 Waverly Place, New York 3, N. Y.

THE FORCE OF IMPACT ON A SPHERE STRIKING A WATER SURFACE

APPROXIMATION BY THE FLOW ABOUT A LENS

Prepared for the
APPLIED MATHEMATICS PANEL
NATIONAL DEFENSE RESEARCH COMMITTEE
By the
Applied Mathematics Group
New York University

This document contains information affecting the National Defense of the United States within the meaning of the Espionage Act, U. S. C. 50; 31 and 32. Its transmission or the revelation of its contents in any manner to an unauthorized person is prohibited by law.

February 1945

CONFIDENTIAL

Prepared under
Contract OEMsr-945

Approved for distribution
Warren Weaver
Chief, Applied Mathematics Panel

Distribution List

AMP Report 42.1R

1 - 8	Office of the Executive Secretary, OSRD
9 - 27	Liaison Office, OSRD
28	War Department Liaison Officer with NDRC Att: Douglas Aircraft - M. S. Plesset
29 - 30	Ordnance Research Center, Aberdeen Proving Ground, Md. Att: O. Veblen
31 - 33	Commanding General, Army Air Forces Att: T. von Karman
34 - 37	Chief, Bureau of Ordnance 1 Att: R. S. Burington 1 Att: Comdr. S. Brunauer 1 Att: Lt. Comdr. W. E. Bleick
38 - 39	Office of the Chief of Ordnance 1 Att: G. C. Evans 1 Att: H. M. Morse
40 - 42	Director, David Taylor Model Basin 1 Att: W. H. Bowers 1 Att: E. H. Kennard
43 - 44	Director, Naval Ordnance Laboratory 1 Att: Ensign D. Gilbarg
45	Director, Naval Research Laboratory Att: G. R. Irwin
46 - 47	E. B. Wilson, Chief, Division 2 1 Woods Hole Oceanographic Institute
48	F. L. Hovde, Chief, Division 3 1 Att: L. Slichter
49 - 52	J. T. Tate, Chief, Division 6 1 Att: C. Herring 1 Att: M. Gimprich 1 Att: F. C. Lindvall

53	W. Weaver, Chief, Applied Mathematics Panel
54	T. C. Fry
55	L. M. Graves
56 - 59	R. Courant
60	S. S. Wilks
61	I. S. Sokolnikoff
62	M. Rees
63	Garrett Birkhoff
64	J. G. Kirkwood
65	F. D. Murnaghan

TABLE OF CONTENTS

Page

Preface.. ii

I. Introduction and Summary.............................. 1

II. Mathematical Treatment............................... 11

Bibliography... 47

Plates:

1. Virtual mass of the fluid.......................... 48
2. Impact-drag coefficient............................ 49
3. Average pressure coefficient...................... 50
4. Comparison with the disc approximation....... 51
5. Comparison with the ellipsoid approximation.. 52
6. Comparison with the sphere approximation..... 53

PREFACE

This paper furnishes an explicit mathematical treatment of the impact forces on a projectile with a spherical nose entering water vertically. On the basis of the results obtained, a less technical memorandum will follow stressing the more intuitive physical aspects of the problem. In addition, an extension of the theory to the problem of oblique entry is being considered.

This study, related to work in which the Applied Mathematics Group at New York University has been engaged at the request of the David Taylor Model Basin and of the Naval Bureau of Ordnance, grew out of informal suggestions made by Ensign David Gilbarg of the Naval Ordnance Laboratory. The work was carried out by Dr. Max Shiffman and Dr. Donald C. Spencer of the New York University Group of the Applied Mathematics Panel with the assistance of Mr. H. Goldstein. Expert numerical help was rendered by the Mathematical Tables Project.

R. Courant
Contractor's Technical Representative

I. Introduction and Summary

1. The impact force. The entry of a bomb, torpedo, or mine from air into water takes place in three stages: (i) the initial stage of short duration following contact with the surface and ending with formation of a cavity behind the projectile; (ii) motion through the water with a trailing cavity extending to the surface; (iii) collapse of the cavity and sinking, a stage in which the cavity is a (possibly pulsating) air bubble following the projectile. Since the deceleration experienced by the bomb is generally largest during the impact stage (i), it is important to obtain a quantitative estimate of the impact force for the purpose of determining possible damage to the mechanism. In this report we are concerned solely with the first phase of the entry.

Furthermore, we suppose that the nose of the projectile is spherical in shape and that the initial impact with the water surface is vertical.

The upward force P acting on the sphere in the impact stage can be expressed in terms of a dimensionless impact-drag coefficient C_p. Let A be the radius of the sphere, U_o its velocity on impact (supposed vertical), and ρ the density of water. Then the impact force P is conveniently expressed as

$$P = \frac{1}{2}\rho U_o^2 \cdot \pi A^2 \cdot C_p$$

where C_p is the "impact-drag coefficient". The coefficient C_p depends on the time - it is zero at the instant of impact,

rapidly increases to a maximum value, and then decreases. It is the main object of this report to determine C_p, and in particular the maximum value of C_p. The result is:

$$\text{maximum value of } C_p = .95.$$

The maximum occurs when the lowest point of the sphere is about one quarter of a radius past the original level of the water surface. At any time t let B be the distance from the lowest point of the sphere to the original level of the water (see Fig. 1). The graph of C_p as a function of B/A is shown in plate 2. (Plates are placed at the end of the report.)

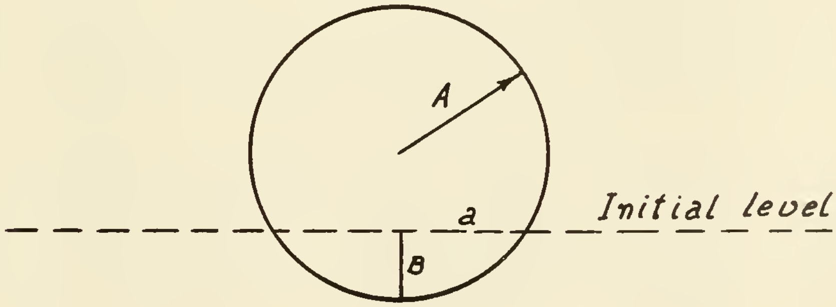

Figure 1

Behind and alongside a rapidly moving projectile entering the water, a cavity is soon formed. It is known for the case of a sphere that this cavity is formed when $\frac{B}{A}$ is somewhere between $\frac{1}{4}$ and 1. Thus the graph of plate 2 should certainly not be used for $\frac{B}{A}$ larger than 1, i.e. when more than half the sphere is submerged. It may be

pointed out, however, that plate 2 is valid for the whole range of $\frac{B}{A}$ if no cavity is formed, which occurs if the initial velocity of the sphere is small.

From the standpoint of damage it is also of interest to know the average pressure $\bar{p}$ acting on the portion of the sphere in contact with the water. At any time t let a be the radius of the circle of intersection of the sphere with the initial level of the water surface (see Fig. 1). Then

$$\bar{p} = \frac{P}{\pi a^2} = \frac{1}{2}\rho U_o^2 \cdot K_p$$

where $K_p = \frac{A^2}{a^2} C_p$. The dependence of K_p on $\frac{B}{A}$ is shown in plate 3. It is noteworthy that the value of K_p at the initial contact of the sphere with the water is infinite. (Actually the compressibility of the water eases the entry somewhat, and the initial pressure $\bar{p}$ is $\rho c U_o$ instead of infinity, where c is the speed of sound in water.)

2. Approximation by flow about a lens. Consider the flow produced in the water as a result of the entry of the sphere. As the sphere penetrates the surface, the free surface no longer remains plane. The water rises slightly and spurts are formed running up the sides of the sphere. The exact shape of the surface is difficult to determine; estimates of the shape and its influence on the impact coefficient will be presented in a separate memorandum. In the present report we shall neglect the motion of the surface and likewise neglect squares of velocities on the surface. The boundary condition on the free surface is then $\phi = 0$, where ϕ is the velocity potential describing the flow. The potential flow can then be extended to the infinite space on both sides of

the free surface, and the flow at each instant corresponds to the flow about a symmetrical lens as indicated in Fig. 2. It is the flow about a lens which forms the main mathematical contribution of this report. It will be determined by explicit mathematical formulae. The method is based on one used by A. Sommerfeld in the theory of diffraction of light and might be useful in the analysis of other hydrodynamical and sound phenomena.

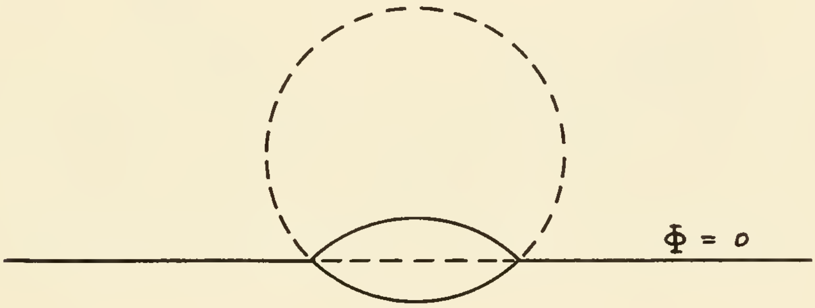

Figure 2

As said before, the flow about the lens provides only a first approximation to the actual flow. This approximation is poor near the edge of the lens because the water streams along the back surface of the lens. In the actual flow the water cannot penetrate the remainder of the sphere and rises instead along its sides.

3. Exact formulation on the basis of the momentum equation.

Let $B = B(t)$ be the distance at time t of the lowest point of the sphere from the initial surface level. Let

$$\dot{B}\Phi(x,y,z;t)$$

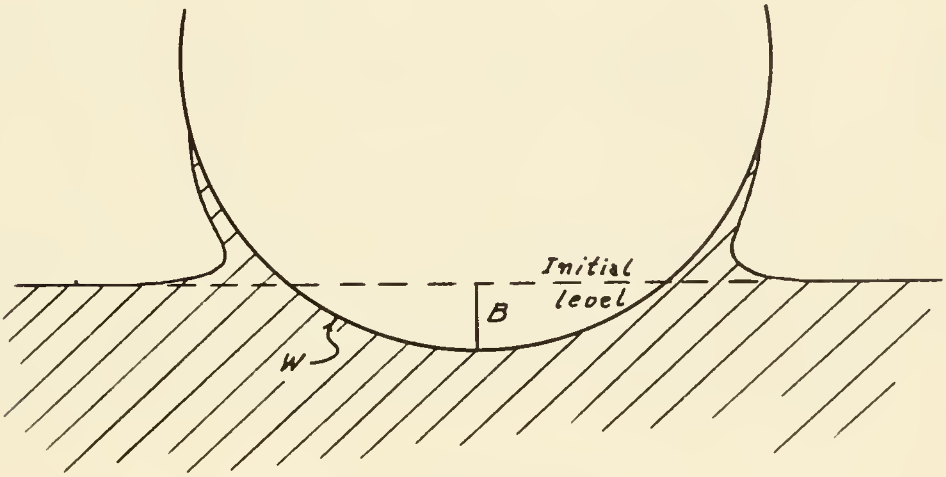

Figure 3

be the velocity potential describing the flow at the instant t. Here $\dot{B} = \frac{dB}{dt}$, and x,y,z are rectangular coordinates, the z-axis being vertical and $z \leq 0$ being the half space initially occupied by the water. The vertically downward momentum of the water is

$$(3.1) \qquad \rho\dot{B}\iiint\frac{\partial\Phi}{\partial z}\,dxdydz = \rho\dot{B}\iint_{W+S}\Phi\,dxdy - \rho\dot{B}L.$$

Here W is the wetted portion of the sphere, S is the free surface, and L is defined to be the limit of the integral

$$\iint \Phi dxdy$$

extended over the submerged portion H of a large spherical membrane the radius of which tends to infinity.

The external forces acting on the fluid contained in the membrane H are: (i) the downward force of magnitude P exerted by the sphere; and (ii) the upward force exerted on H by the pressure of the fluid external to it. (The resultant force due to the constant atmospheric pressure is zero. The only effect of gravity is the buoyancy, which is negligible compared to the impact force P.) The force (ii) is equal to the time rate of change of the term $-\rho\dot{B}L$ in (3.1), as may be seen from Bernoulli's equation. Since the resultant of the external forces is equal to the time rate of change of the momentum (3.1), we therefore have

$$P = \frac{d}{dt}(M\dot{B}) \tag{3.2}$$

where

$$M = \rho \iint_{W+S} \Phi dxdy. \tag{3.3}$$

The quantity M may be considered to be the effective "momentum mass" of the water.

Let M_o be the mass of the incoming projectile. Since

$$-P = \frac{d}{dt}(M_o\dot{B}) , \tag{3.4}$$

we obtain from (3.2)

$$(3.5) \qquad (M + M_o)\dot{B} = M_o U_o \ , \text{ or } \dot{B} = \frac{U_o}{1+\mu}$$

where $\mu = \frac{M}{M_o}$. Equation (3.5) expresses conservation of momentum.

From (3.4) and (3.5), it follows that

$$(3.6) \qquad P = \frac{\frac{dM}{dB}}{1+\mu} \dot{B}^2 = \frac{\frac{dM}{dB}}{(1+\mu)^3} U_o^2 \ .$$

Introducing the dimensionless quantities

$$(3.7) \qquad m = \frac{M}{\frac{1}{2}\pi\rho A^3} \ , \quad b = \frac{B}{A} \ ,$$

we may write

$$(3.8) \qquad P = \frac{1}{2}\rho U_o^2 \cdot \pi A^2 \cdot C_p$$

where

$$(3.9) \qquad C_p = \frac{\frac{dm}{db}}{(1+\mu)^3} \ .$$

For incoming projectiles of large mass compared to the mass of water displaced by the hemispherical nose, μ may be neglected. Then the impact-drag coefficient C_p is merely $\frac{dm}{db}$.

The problem is thus to find M or, since the exact flow is difficult to determine, a reasonable approximation to M.

The result obtained in the present paper is: the dimensionless virtual mass m and the impact-drag coefficient $\frac{dm}{db}$ depend on the depth of penetration b in the way indicated in plates 1 and 2. The maximum value of $\frac{dm}{db}$ is .95, and it occurs for $b = .24$.

It is possible to use an energy equation in place of a momentum equation, but this would require a more detailed analysis of the free surface. For the spurts that run up the side of the sphere may carry considerable energy, whereas the vertical momentum they carry is small. Also, there may be energy losses due to sound waves in the water and elastic vibrations of the projectile.

4. Comparison of lens flow with disc and ellipsoid flows.

Various writers (see references [2], [4] and [5] in the bibliography at the end of the report) calculate C_p on the basis of the following assumption: the entering body at each instant of time t is replaced by its cross section at the surface (assumed to be the initial surface) and the virtual mass M is taken to be that due to the flow about this disc. If the disc has a radius a, the virtual mass is, from classical hydrodynamics, equal to

$$\frac{4}{3}\rho a^3 .$$

The dimensionless virtual mass m_1 is then

$$m_1 = \frac{\frac{4}{3}\rho a^3}{\frac{1}{2}\pi\rho A^3} = \frac{8}{3\pi}[b(2-b)]^{3/2} ,$$

and the impact-drag coefficient $\frac{dm_1}{db}$ is

$$\frac{dm_1}{db} = \frac{8}{\pi}(1-b)\sqrt{b(2-b)}$$

A comparison of this approximation with the lens flow approximation used in this paper is given in plate 4. The agreement is fair. The maximum of $\frac{dm_1}{db}$ in the disc approximation is 1.27 compared to .95 for the more accurate lens.

Instead of a disc, consider an ellipsoid of revolution which fits the lens as shown in the diagram, with semi-axes a, a, B. The flow about such an ellipsoid would seem to be a better approximation.

The flow about an ellipsoid is classical (see [1], pages 456 and 457). Write $\gamma = \frac{B}{a}$ and assume that $0 \leq \gamma < 1$.

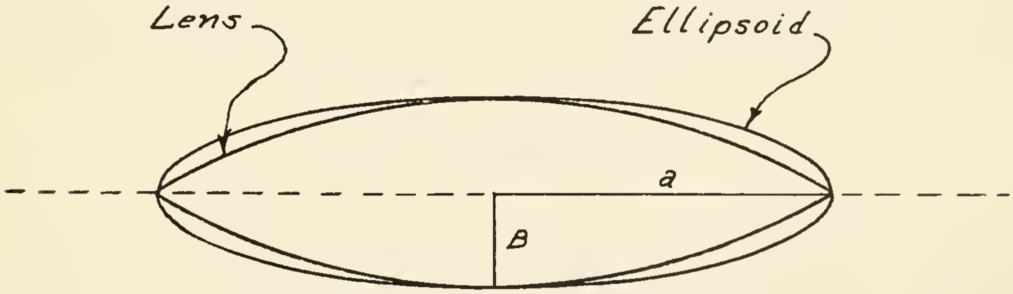

Figure 4

The dimensionless virtual mass m_2 then is

$$m_2 = \frac{4}{3} b^2 (2-b) \frac{\alpha_o}{2 - \alpha_o}$$

where

$$\alpha_o = \frac{2}{1-\gamma^2} \left(1 - \frac{\gamma}{\sqrt{1-\gamma^2}} \operatorname{arc} \cos \gamma \right) \qquad (0 < \operatorname{arc} \cos \gamma \leq 1) ,$$

and the impact-drag coefficient is

$$\frac{dm_2}{db} = - \frac{4}{3} b(3b - 4) \frac{\alpha_o}{2 - \alpha_o} + \frac{8}{3} \sqrt{b(2-b)} \left(\frac{\gamma}{2 - \alpha_o} \right)^2 \frac{d\alpha_o}{d\gamma} .$$

It is seen from plate 5 that the agreement with the lens flow is better than that of the disc. The maximum of $\frac{dm_2}{db}$ in the ellipsoid approximation is 1.1, compared to .95 for the lens.

As another possible approximation, take a sphere with center at the center of the lens and radius equal to a. The virtual mass is $\frac{1}{3} \pi \rho a^3$, and the impact-drag coefficient is

$$\frac{dm_3}{db} = (2-2b)(2b-b^2)^{1/2} .$$

A graph of $\frac{dm_3}{db}$ is given in plate 6, and it is seen to be a better approximation in the neighborhood of the maximum than the corresponding quantity for either the disc or the ellipsoid.

We have been concerned in this paper only with vertical entry. However, for oblique entry it would seem desirable to replace the lens by an ellipsoid and then to solve this somewhat easier problem.

II. Mathematical Treatment.

5. Preliminary remarks. The flow pattern of the fluid at the time t is described by a velocity potential

$$\dot{B}\phi(x,y,z;t)$$

which satisfies the Laplace equation

$$\phi_{xx} + \phi_{yy} + \phi_{zz} = 0$$

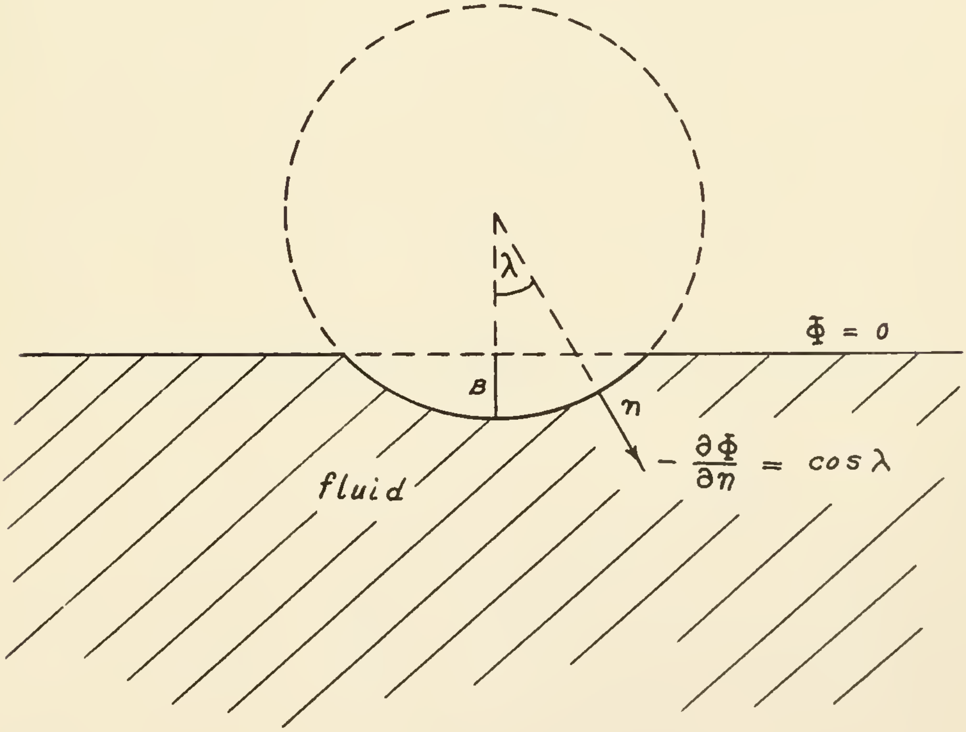

Figure 5

together with the following boundary conditions:

(a) On the sphere, the negative of the normal derivative of $\dot{B}\Phi$ is equal to the component of the velocity of the sphere along the normal, or

$$-\dot{B}\frac{\partial\Phi}{\partial n} = \dot{B}\cos\lambda .$$

(b) By virtue of the assumptions made in Part I, Sect. 2, Φ vanishes on the plane $z = 0$.

To see how to construct this potential function Φ, consider first the case in which the sphere is completely immersed in the water and moving vertically (see Fig. 5). A classical method of constructing the desired potential function is by

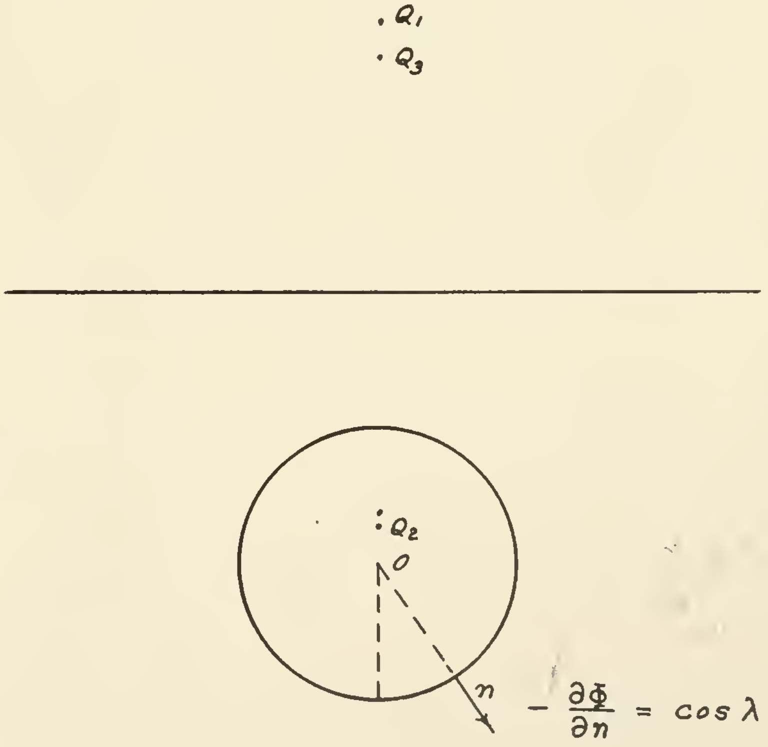

Figure 6

the method of images (see [1], page 420). Suppose that the free surface were not present. The flow produced by a sphere moving in an infinite body of fluid is that created by a dipole of suitable strength placed at the center O of the sphere. This satisfies the boundary condition (a) on the sphere. However, because of the presence of the free surface, the boundary condition (b) on the plane $z = 0$ is violated. To satisfy (b) introduce the image of the dipole relative to the plane $z = 0$, which is a dipole of equal strength at the reflected point Q_1. The condition (a) on the sphere is now violated, and to remedy it introduce the image of the latter dipole relative to the sphere. This image is a dipole of suitable strength at the inverse point Q_2. Indefinite continuation of this process leads to a potential function which satisfies both the boundary conditions (a) and (b).

We shall apply a generalization of the above process to the case where the sphere intersects the free surface (see Fig. 5). The process as it stands leads to a serious difficulty, namely that some of the successive images lie in the fluid below the sphere, thus creating dipoles (singularities) inside the fluid which violate the assumptions of the problem. For example, in Fig. 5 (where $B < \frac{A}{2}$), the image of the dipole at the center of the sphere relative to the plane $z = 0$ introduces a dipole in the fluid.

The difficulty may be overcome by using multi-valued dipoles, the images of which lie in the various replicas ("sheets") of a Riemann space and do not give rise to singularities in that portion of the space in which we are interested. The construction of the multi-valued dipoles is based on the method used by A. Sommerfeld in his classical work on the theory of diffraction (see [3]).

We describe the Riemann space in the next section, and discuss the multi-valued dipoles in sections 7-9. The potential

function ϕ satisfying the boundary conditions (a) and (b) is constructed in section 10, the final formula being (10.11).

The velocity potential ϕ, extended to the whole space by reflection in the plane $z = 0$, describes the flow about a symmetrical lens. In Appendix A we discuss the flow about an asymmetrical lens formed by the intersection of any two spheres.

Finally, if the sphere is entirely below the surface $z = 0$ and does not intersect it, the construction of ϕ is classical (as stated above). In Appendix B, however, it is noted that the potential function can also be obtained merely by replacing some of the real quantities occurring in our formulas by purely imaginary ones.

6. The coordinate system and the Riemann space. We select a coordinate system which fits the problem better than either the ordinary rectangular or cylindrical system. It is obtained from bipolar coordinates in the plane (see [1], page 165) by rotation about an axis.

Let r,z be ordinary rectangular coordinates in the plane. Introduce in place of r,z the bipolar coordinates σ, ψ defined, in complex terminology, as follows:

$$(6.1)\quad \sigma - i\psi = \log \frac{r + iz + a}{r + iz - a}, \quad \text{or} \quad r + iz = ai \cot \tfrac{1}{2}(\psi + i\sigma).$$

Geometrically, σ is the logarithm of the ratio of the distances from the two points $-a$ and a on the real axis and ψ is the angle subtended by the line joining these two points (see Fig. 7).

We observe that the curve $\psi =$ constant is a circular arc connecting the points P_1 and P_2. The curve σ = constant

is a circle with center on the real axis and with the points P_1 and P_2 as mutually inverse points.

The value of ψ on the upper side of the line segment P_1P_2 is π ; the value of ψ on the lower side is $-\pi$. The simple plane is obtained by identifying these two values of the angle ψ . But if the angle ψ is allowed to vary outside the range $-\pi \leq \psi \leq \pi$, and if values of ψ differing by 2π are not identified, we obtain a Riemann surface with P_1 and P_2 as branch points. The Riemann surface which we consider is the infinite-sheeted one in which ψ is permitted to take any value from $-\infty$ to $+\infty$ with no identifications.

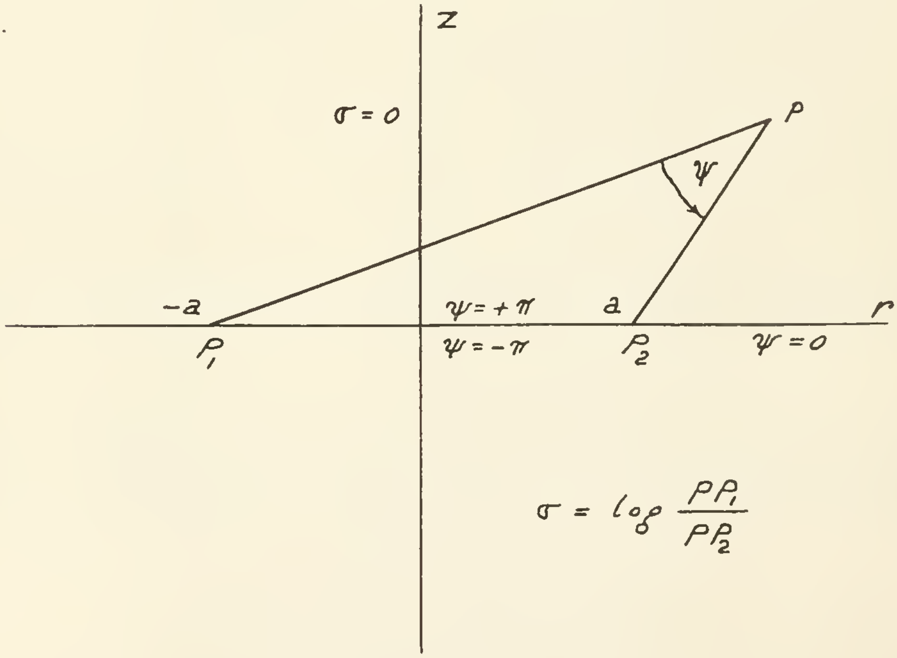

Figure 7

A system of coordinates in space is obtained by rotating the plane about the z-axis. Let θ be the angle of rotation. The space coordinates σ, ψ, θ are called toroidal (because the surface σ = constant is a torus).

To the Riemann surface discussed above there corresponds in space an infinite-fold Riemann space. The branch points at $\pm a$ are replaced in space by the circular branch curve $r = a$, $z = 0$, and the cut line joining P_1 and P_2 is replaced by a cut surface $r < a$, $z = 0$ across which the replicas (or "sheets") of the space are joined.

The equation (6.1) defining bipolar coordinates can be expressed in real form as follows:

$$(6.2) \qquad r = a\,\frac{\sinh\sigma}{s-\tau}\,, \qquad z = a\,\frac{\sin\psi}{s-\tau}$$

where $s = \cosh\sigma$, $\tau = \cos\psi$. The element of length in space is

$$(6.3) \quad dz^2 + dr^2 + r^2 d\theta^2 = \frac{a^2}{(s-\tau)^2}\,(d\sigma^2 + d\psi^2 + \sinh^2\sigma\, d\theta^2).$$

We observe finally that the points (σ, ψ_0, θ) and $(\sigma, \psi_0', \theta)$ are inverse with respect to the spherical cap ψ = constant = c provided that

$$(6.4) \qquad \psi_0 + \psi_0' = 2c.$$

For the mapping in which the point (σ, ψ) goes into $(\sigma, \psi + c)$, where c is a fixed real quantity, is a linear transformation of any plane θ = constant into itself. Since the above statement about inverse points is true when c = 0, it is true generally because it is invariant to the linear transformations.

7. Dipoles. In this section we obtain the expression for a dipole in toroidal coordinates.

The inverse distance between a point on the z-axis $\sigma = 0$ at $\psi = \psi_o$ and an arbitrary point (σ, ψ, θ) of the space is, from (6.1)

$$(7.1)\quad \frac{1}{R} = \frac{1}{|(r + iz) - (iz_o)|} = \frac{\left|\sin\frac{\psi_o}{2}\right|}{a} \sqrt{\frac{s - \tau}{s - \cos(\psi - \psi_o)}} \;.$$

This represents a unit pole on the z-axis ($\sigma = 0$) at the point $z = z_o = a \cot \frac{\psi_o}{2}$. Instead of (7.1) we introduce the function

$$(7.2)\qquad p_{\psi_o} = \sin\frac{\psi_o}{2} \sqrt{\frac{s - \tau}{s - \cos(\psi - \psi_o)}} \;,$$

which represents a pole of strength ± a .

A dipole at the same point is obtained by differentiating (7.2) with respect to z_o. However we shall find it more convenient to use a dipole of suitable strength, namely

$$(7.3)\quad q_{\psi_o}(\sigma, \psi) = -\frac{a^2}{2} \csc^3\frac{\psi_o}{2} \frac{\partial}{\partial z_o}(p_{\psi_o}) = a \csc\frac{\psi_o}{2} \frac{\partial}{\partial \psi_o}(p_{\psi_o})$$

$$= \frac{a}{2}\left[\frac{(s-\tau)^{1/2} \sin(\psi - \psi_o)}{[s - \cos(\psi - \psi_o)]^{3/2}} + \cot\frac{\psi_o}{2} \frac{(s - \tau)^{1/2}}{[s - \cos(\psi - \psi_o)]^{1/2}} \right].$$

This function is a dipole of strength $-\frac{a^3}{2}\left|\csc^3\frac{\psi_o}{2}\right|$ situated at the point $z = z_o = a \cot\frac{\psi_o}{2}$ on the z-axis.

The Stokes' stream function t_{ψ_0} corresponding to q_{ψ_0} is (see [1], Chapter XV, especially page 414):

$$(7.4) \quad t_{\psi_0} = \frac{a^3}{2} \left|\csc^3 \frac{\psi_0}{2}\right| \frac{r^2}{R^3} = \frac{1}{2} a^2 \frac{\sinh^2 \sigma}{(s-\tau)^{1/2}[s-\cos(\psi - \psi_0)]^{3/2}} .$$

The functions q_{ψ_0} and t_{ψ_0} are connected by the linear differential equations

$$(7.5) \quad \begin{aligned} \frac{\partial q_{\psi_0}}{\partial \sigma} &= -\frac{1}{r} \frac{\partial t_{\psi_0}}{\partial \psi} \\ \frac{\partial q_{\psi_0}}{\partial \psi} &= \frac{1}{r} \frac{\partial t_{\psi_0}}{\partial \sigma} . \end{aligned}$$

We wish to find the image of the dipole q_{ψ_0} in the spherical cap ψ = constant = c; that is, we wish to find a potential function Φ such that the normal derivative of $q_{\psi_0} + \Phi$ is zero on $\psi = c$. This condition is equivalent to the statement that the sum of the corresponding Stokes' stream functions is constant over the cap. We shall show that the image is $-q_{\psi_0'}$ where $\psi_0 + \psi_0' = 2c$, or $c - \psi_0 = -(c - \psi_0')$. The functions q_{ψ_0} and $q_{\psi_0'}$ are dipoles situated on the z-axis at the points given by $\psi = \psi_0$ and $\psi = \psi_0'$, and these points are mutually inverse relative to the spherical cap $\psi = c$. (See (6.4).)

The Stokes' stream function for the sum $q_{\psi_0} - q_{\psi_0'}$ is $t_{\psi_0} - t_{\psi_0'}$ which vanishes on $\psi = c$ by (7.4) since $\cos(c - \psi_0) = \cos(c - \psi_0')$. Thus the normal derivative of $q_{\psi_0} - q_{\psi_0'}$ is zero on $\psi = c$. (This is the reason for taking a dipole of strength $-\frac{a^3}{2}\left|\csc^3 \frac{\psi_0}{2}\right|$ as the basic dipole q_{ψ_0}. The stream function then has a simple form and leads to a simple image result.)

8. Multi-valued dipoles. The construction of our multi-valued dipoles will be based on the method of Sommerfeld referred to above. Since ψ_0 is involved in an analytic way in p_{ψ_0} and q_{ψ_0}, these functions of σ and ψ still satisfy the potential equation when ψ_0 is replaced by a complex number ξ. They may be regarded as representing a pole or dipole respectively, situated at the "complex point" $\sigma = 0$, $\psi = \xi$. Also t_ξ is the stream function corresponding to q_ξ, since the differential equations (7.5) are still satisfied when ξ is complex.

As functions of ξ in the complex ξ-plane, p_ξ, q_ξ, t_ξ are multi-valued and have branch points at the zeros of $s-\cos(\psi-\xi)$, that is at $\xi = \psi \pm i\sigma + 2k\pi$ where $k=0, \pm 1, \pm 2, \dots$.

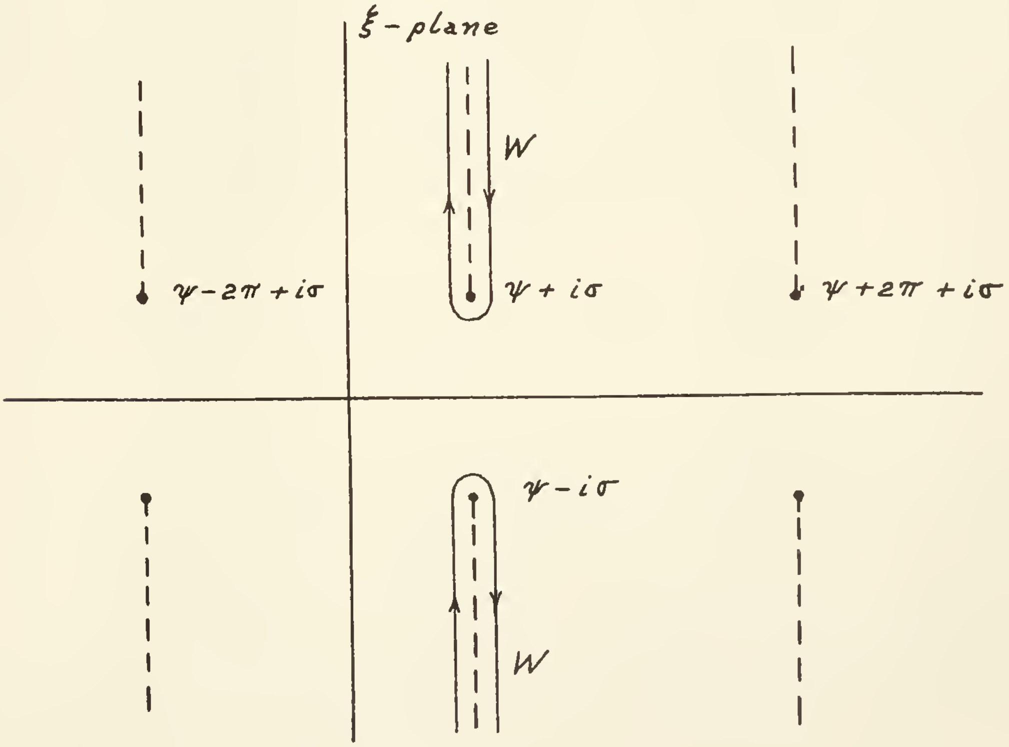

Figure 8

Cut the ξ-plane by vertical lines proceeding from the branch points to ∞ as shown in the diagram (Fig. 8). The functions p_ξ, q_ξ, t_ξ are now single-valued in this cut ξ-plane and take opposite signs on the opposite sides of each cut. We define $[s-\cos(\psi-\xi)]^{1/2}$ to be positive when ξ is real.

The basic multi-valued dipole situated at a (real) point $\sigma = 0$, $\psi = \psi_0$ on the z-axis of our infinite-sheeted Riemann space is defined as follows:

$$(8.1) \qquad q_{\psi_0}^{(\infty)}(\sigma,\psi) = \frac{1}{2\pi i}\int_W q_\xi \frac{1}{\xi-\psi_0}\, d\xi$$

where the path W of integration is the two-branched path indicated in the diagram. The function $q_{\psi_0}^{(\infty)}(\sigma,\psi)$ is a potential function since differentiations can be performed under the integral sign, the path W being temporarily fixed.

(For an n-sheeted Riemann space in which values of the angle ψ differing by $2n\pi$ would be identified, the corresponding n-valued dipole $q_{\psi_0}^{(n)}(\sigma,\psi)$ is

$$(8.2) \qquad q_{\psi_0}^{(n)}(\sigma,\psi) = \frac{1}{2\pi i}\int_W q_\xi \cdot \frac{1}{2n}\cot\frac{\xi-\psi_0}{2n}\, d\xi \quad .$$

Since $\cot\frac{\xi-\psi_0}{2n}$ is periodic in ξ of period $2n\pi$, and q_ξ is periodic of period 2π, it is easy to see that $q_{\psi_0}^{(n)}(\sigma,\psi)$ is periodic in ψ of period $2n\pi$.)

We now briefly describe the properties of $q_{\psi_0}^{(\infty)}(\sigma,\psi)$. (A similar description applies to $q_{\psi_0}^{(n)}(\sigma,\psi)$.) On account of the pole of the integrand in (8.1) at ψ_0 one sees, by the Cauchy residue theorem, that

$$(8.3) \qquad q_{\psi_0}^{(\infty)} - q_{\psi_0}(\sigma,\psi)$$

is regular as $\sigma \to 0$ and $\psi \to \psi_0 (\psi_0 \neq 2j\pi)$. Thus $q^{(\infty)}_{\psi_0}$ behaves like a dipole near $\sigma = 0$, $\psi = \psi_0$. But $q^{(\infty)}_{\psi_0}(\sigma,\psi)$ is regular near $\sigma = 0$, $\psi = \psi_0 + 2k\pi$, $k = \pm 1, \pm 2, \ldots$, since the integrand is regular at these points.

In addition there are still the poles of q_ξ itself at $\xi = 2k\pi$, $k = 0, \pm 1, \pm 2, \ldots$ due to the presence of the term $\cot \frac{\xi}{2}$ (see (7.3)). One easily sees that

$$(8.4) \qquad q^{(\infty)}_{\psi_0} \to \frac{a}{2k\pi - \psi_0}$$

as $\sigma \to 0$ and $\psi \to 2k\pi$, $k = 0, \pm 1, \pm 2, \ldots$ $(\psi_0 \neq 2j\pi)$. Thus, the function $q^{(\infty)}_{\psi_0}$ is not simply a dipole at ψ_0 but it has certain non-vanishing values at ∞ $(\sigma = 0, \psi = 2k\pi)$ in the various sheets and has no other singularities. (A constant value at ∞ may be thought of as a pole at ∞. If in the definition of q_ξ the term $\cot \frac{\xi}{2}$ were replaced by $\cot \frac{\psi_0}{2}$, the resulting function in (8.1) would be zero at the points at ∞; this would be a simple dipole).

In the above we have implicitly assumed that ψ_0 is not a multiple of 2π, for then the integrand in (8.1) has a multiple pole. Consider, for example, $q^{(\infty)}_0(\sigma,\psi)$. The integrand in (8.1) has a double pole at $\xi = 0$, and the residue there is

$$\frac{a}{2}\frac{\sin\psi}{s-\tau} + a\left[\frac{\partial}{\partial\xi}\left(\frac{s-\tau}{s-\cos(\psi-\xi)}\right)^{1/2}\right] = a\,\frac{\sin\psi}{s-\tau} = z \quad .$$

Therefore

$$(8.5) \qquad q^{(\infty)}_0(\sigma,\psi) - z \to 0$$

as $\sigma \to 0$ and $\psi \to 0$, and so $q^{(\infty)}_0(\sigma,\psi)$ behaves like z near

the point at ∞ in the first sheet. A similar analysis applies to $q^{(\infty)}_{2k\pi}(\sigma,\psi)$.

In the n-sheeted case, it is of interest to consider the special case $n = 1$ where we are in the original single-sheeted space. The integrand in (8.2) is of period 2π, and a simple analysis yields

$$q^{(1)}_{\psi_0}(\sigma,\psi) = q_{\psi_0}(\sigma,\psi) - \frac{a}{2}\cot\frac{\psi_0}{2} \qquad \psi_0 \neq 0 \,, \tag{8.6}$$

so $q^{(1)}_{\psi_0}$ differs from an ordinary dipole q_{ψ_0} by a constant. If in (8.6) we now let $\psi_0 \to 0$, we obtain

$$q^{(1)}_{\psi_0}(\sigma,\psi) \to z \,.$$

It may also be verified directly that

$$q^{(1)}_{0}(\sigma,\psi) = z \,. \tag{8.7}$$

9. *Inversion of multi-valued dipoles*. It is well-known that in ordinary space the image of a dipole with respect to a sphere is another dipole situated at the inverse point. In this section the theorem will be extended to multi-sheeted spaces.

Theorem 9.1. The function $q^{(\infty)}_{\psi_0}(\sigma,\psi) - q^{(\infty)}_{\psi_0'}(\sigma,\psi)$ has vanishing normal derivative on the spherical cap $\psi = \text{constant} = c$ if $\psi_0 + \psi_0' = 2c$.

Proof: Because the relations connecting stream function and potential function are linear, the stream function $t^{(\infty)}_{\psi_0}(\sigma,\psi)$ corresponding to $q^{(\infty)}_{\psi_0}(\sigma,\psi)$ is

$$t^{(\infty)}_{\psi_0}(\sigma,\psi) = \frac{1}{2\pi i}\int_W t_\xi \cdot \frac{1}{\xi - \psi_0}\,d\xi$$

where t_ξ is the stream function corresponding to q_ξ, obtained from (7.4) by replacing ψ_0 by ξ. It is required to show merely that $t^{(\infty)}_{\psi_0}(\sigma,\psi) - t^{(\infty)}_{\psi_0'}(\sigma,\psi)$ is constant on $\psi = c$.

It is more convenient to introduce a new complex variable ζ defined by $\xi - \psi = \zeta$. Then

$$q_\xi = \frac{a}{2}\left[- \frac{(s-\tau)^{1/2}\sin\zeta}{(s-\cos\zeta)^{3/2}} + \cot\frac{\zeta+\psi}{2}\,\frac{(s-\tau)^{1/2}}{(s-\cos\zeta)^{1/2}}\right] \tag{9.1}$$

$$t_\xi = \frac{1}{2}a^2\,\frac{\sinh^2\sigma}{(s-\tau)^{1/2}(s-\cos\zeta)^{3/2}} \tag{9.2}$$

and

$$q^{(\infty)}_{\psi_0}(\sigma,\psi) = \frac{1}{2\pi i}\int_{W'} q_\xi \cdot \frac{1}{\zeta+\psi-\psi_0}\,d\zeta \tag{9.3}$$

$$t^{(\infty)}_{\psi_0}(\sigma,\psi) = \frac{1}{2\pi i}\int_{W'} t_\xi \cdot \frac{1}{\zeta+\psi-\psi_0}\,d\zeta \tag{9.4}$$

where W' is the path in the ζ-plane shown in the figure.

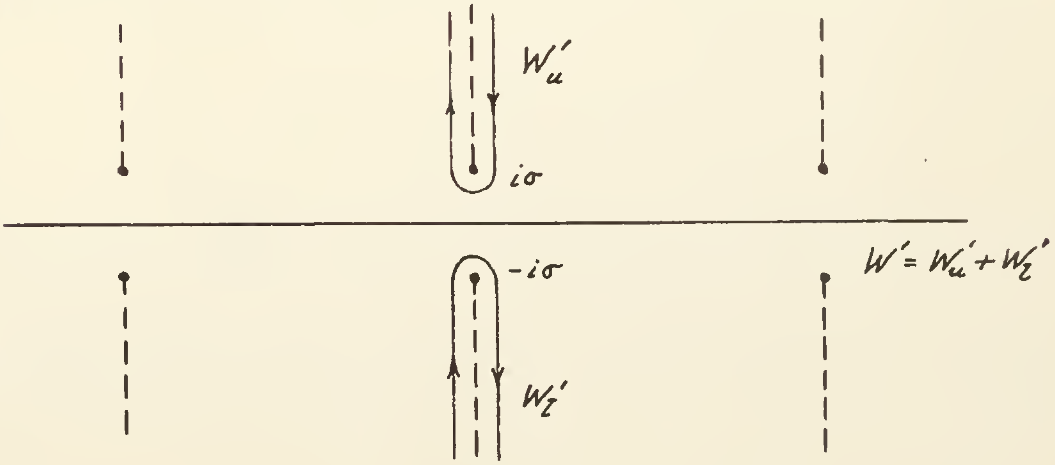

Figure 9

By the symmetry of the path W', the lower path W'_ℓ is obtained from the upper path W'_u by replacing ζ by $-\zeta$. The function t_ξ is by (9.2) an even function of ζ. Therefore (9.4) can be written in the form

$$(9.5) \quad t^{(\infty)}_{\psi_0}(\sigma,\psi) = \frac{1}{2\pi i}\int_{W'_u} t_\xi \cdot \left(\frac{1}{\zeta + (\psi - \psi_0)} + \frac{1}{\zeta - (\psi - \psi_0)} \right) d\zeta .$$

Likewise for $t^{(\infty)}_{\psi'_0}(\sigma,\psi)$. Evaluating at $\psi = c$ and noting that the hypothesis $\psi_0 + \psi'_0 = 2c$ can be written $c - \psi_0 = -(c - \psi'_0)$, equation (9.5) shows immediately that $t^{(\infty)}_{\psi_0}(\sigma, c) = t^{(\infty)}_{\psi'_0}(\sigma, c)$, and the theorem is proved.

Theorem 9.2. The function $q^{(\infty)}_{\psi_0}(\sigma,\psi) + q^{(\infty)}_{-\psi_0}(\sigma,\psi)$ vanishes on $\psi = 0$. In particular $q^{(\infty)}_0(\sigma,\psi)$ vanishes on $\psi = 0$.

Proof: For $\psi = 0$ the function q_ξ is an odd function of ζ by (9.1). The same argument as in the proof of theorem 9.1, applied to (9.3), yields $q^{(\infty)}_{\psi_0}(\sigma,0) = -q^{(\infty)}_{-\psi_0}(\sigma,0)$. The second statement of the theorem is an immediate consequence of the first one.

10. Construction of the potential function. We are now prepared to apply the method of images discussed in Section 5. The desired potential Φ is regular at ∞ $(\sigma = 0, \psi = 0)$ and satisfies the following boundary conditions:

$$(10.1) \qquad \Phi = 0 \quad \text{on} \quad \psi = 0$$

$$(10.2) \qquad -\frac{\partial \Phi}{\partial n} = \cos \lambda = -\frac{\partial z}{\partial n} \quad \text{on} \quad \psi = -\beta .$$

The potential function z satisfies (10.1) and (10.2) but is not regular at ∞. Set

$$(10.3) \qquad V = \Phi - z$$

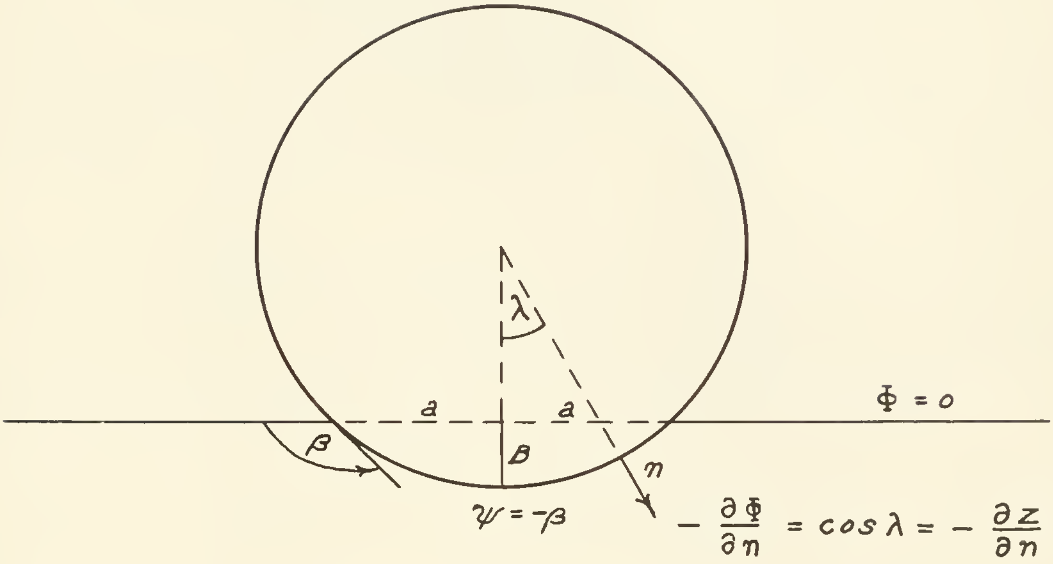
λ
a
a
β
β
n
$\Phi = 0$
$\psi = -\beta$
$-\frac{\partial \Phi}{\partial n} = \cos\lambda = -\frac{\partial z}{\partial n}$

Figure 10

Then V is a potential function satisfying the following conditions:

(10.4) $$V = 0 \quad \text{on} \quad \psi = 0$$

(10.5) $$-\frac{\partial V}{\partial n} = 0 \quad \text{on} \quad \psi = -\beta$$

and

(10.6) V behaves like $-z$ at ∞.

(The potential function V corresponds to the flow about a fixed lens, the fluid having unit velocity at ∞.)

We shall construct V by the method of images, using the infinite-sheeted Riemann space described by $0 \leq \sigma < \infty$, $-\infty < \psi < +\infty$. (It may be pointed out that if the angle $\beta = \frac{\pi n}{2q}$ where n, q are integers, it would be sufficient to use an n-sheeted Riemann space in place of the infinite-sheeted one.)

To construct V, first start with $-\overset{(\infty)}{q}_0(\sigma,\psi)$ which has the correct behavior (10.6) as $\sigma \to 0$, $\psi \to 0$ (by (8.5), and satisfies (10.4). To satisfy (10.5), one must add $\overset{(\infty)}{q}_{-2\beta}(\sigma,\psi)$ by theorem 9.1; to satisfy (10.4), one must now add $\overset{(\infty)}{q}_{2\beta}(\sigma,\psi)$ by theorem 9.2; etc. The result is

$$(10.7) \qquad V(\sigma,\psi) = \sum_{k=-\infty}^{+\infty} (-1)^{k+1} \overset{(\infty)}{q}_{2k\beta}(\sigma,\psi)$$

where the sum means $\lim_{N\to\infty} \sum_{k=-N}^{N}$. We demonstrate the convergence of this sum below by evaluating it. We may write (10.7) in the forms

$$(10.8) \quad V(\sigma,\psi) = -\overset{(\infty)}{q}_0(\sigma,\psi) + \sum_{k=1}^{\infty} (-1)^{k+1} \left[\overset{(\infty)}{q}_{2k\beta}(\sigma,\psi) + \overset{(\infty)}{q}_{-2k\beta}(\sigma,\psi) \right]$$

and

$$(10.9) \qquad V(\sigma,\psi) = \sum_{k=0}^{\infty} (-1)^{k+1} \left[\overset{(\infty)}{q}_{2k\beta}(\sigma,\psi) - \overset{(\infty)}{q}_{-2(k+1)\beta}(\sigma,\psi) \right] .$$

Equation (10.8) shows that (10.4) and (10.6) are satisfied; equation (10.9) that (10.5) is satisfied.

Substituting from (8.2) we obtain

$$V(\sigma,\psi) = \frac{1}{2\pi i} \int_W q_\xi \cdot \left[\sum_{k=-\infty}^{+\infty} (-1)^{k+1} \frac{1}{\xi - 2k\beta} \right] d\xi$$

or

$$(10.10)\quad V = -\frac{1}{2\pi i}\int_{W} q_{\xi}\cdot\frac{\pi}{2\beta}\csc\frac{\pi\xi}{2\beta}\,d\xi = -\frac{1}{2\pi i}\int_{W'} q_{\xi}\cdot\frac{\pi}{2\beta}\csc\frac{\pi}{2\beta}(\psi+\xi)\,d\xi\ .$$

Expressed as a real integral

$$V = \frac{1}{2}A\frac{\sin\beta}{\beta}\int_{\sigma}^{\infty}\sqrt{\frac{s-\tau}{\cosh u - s}}\ \mathrm{Im}\left[\cot\frac{\xi}{2}\csc\frac{\pi\xi}{2\beta} + \frac{\pi}{\beta}\csc\frac{\pi\xi}{2\beta}\cot\frac{\pi\xi}{2\beta}\right]du$$

where $\xi = \psi + iu$. The desired potential function is $\Phi = V + z$ by (10.3). It is easily verified from (8.7) that

$$z = -\frac{A\sin\beta}{\pi}\int_{\sigma}^{\infty}\sqrt{\frac{s-\tau}{\cosh u - s}}\ \mathrm{Im}\left[\csc^{2}\frac{\xi}{2}\right]du \quad (\xi = \psi + iu)\ ,$$

and so we may express the desired potential function as a real integral in the form

$$(10.11)\quad \Phi = \frac{A\sin\beta}{2\pi}\int_{\sigma}^{\infty}\sqrt{\frac{s-\tau}{\cosh u - s}}\cdot\mathrm{Im}\left[\frac{\pi}{\beta}\cot\frac{\xi}{2}\csc\frac{\pi\xi}{2\beta} + \frac{\pi^{2}}{\beta^{2}}\csc\frac{\pi\xi}{2\beta}\cot\frac{\pi\xi}{2\beta} - 2\csc^{2}\frac{\xi}{2}\right]du$$

We observe that the function whose imaginary part appears in the integrand of (10.11) is bounded at $\xi = 0$, and we therefore see directly that $\Phi = 0$ at ∞ ($\sigma = 0$, $\psi = 0$) because the factor $\sqrt{s - \tau}$ vanishes.

11. Virtual mass of the fluid. As stated in Section 2 we neglect the motion of the surface. Then $\Phi = 0$ on the surface S, and the wetted portion W of the sphere is the spherical cap $\psi = -\beta$. By (3.3) the virtual mass of the fluid becomes

$$M = \rho \iint_{\psi=-\beta} \Phi \, dxdy = \rho \iint_{\psi=-\beta} \Phi \cos\lambda \, dS$$

where dS denotes an element of area on $\psi = -\beta$ and λ is the angle indicated in Fig. 10. Since $\cos\lambda = -\frac{\partial z}{\partial n} = -\frac{\partial \Phi}{\partial n}$, we observe that under these circumstances M is also the kinetic-energy virtual mass of the fluid.

Since $\Phi = V + z$ we have

$$M = M_V - M_z \tag{11.1}$$

where

$$M_V = \rho \iint_{\psi=-\beta} V \cos\lambda \, dS \tag{11.2}$$

and

$$M_z = -\rho \iint_{\psi=-\beta} z \, dxdy = \frac{4}{3}\pi\rho A^3 \cos^4\frac{\beta}{2}(2-\cos\beta) \tag{11.3}$$

$$= \frac{1}{3}\pi\rho A^3(2 + 3\cos\beta - \cos^3\beta)$$

by an elementary calculation. In fact M_z is equal to the mass of the fluid displaced by the sphere.

The element of area dS on the spherical cap $\psi = -\beta$ is

$$dS = 2\pi r \frac{a}{s-\tau} d\sigma = 2\pi a^2 \frac{\sinh\sigma \, d\sigma}{(s-\tau)^2} = 2\pi a^2 \frac{ds}{(s-\tau)^2}$$

where $\tau = \cos\beta$. Also $\cos\lambda = -\frac{\partial z}{\partial n} = -\frac{z - z_o}{A}$ where z_o is the z-coordinate of the center of the sphere, and z that

of a point on the surface of the sphere. Thus $z = -a\frac{\sin\beta}{s-\tau}$ and $z_0 = -\cot\beta$ and we have

$$\cos\lambda = -\frac{\partial z}{\partial n} = -\frac{a}{A}\left(\cot\beta - \frac{\sin\beta}{s-\tau}\right) = -\sin\beta\cdot\left(\cot\beta - \frac{\sin\beta}{s-\tau}\right)(0 \leq \beta \leq \pi).$$

Hence

$$(11.4)\quad M_V = -2\pi\rho a^2\int_1^\infty V(\sigma,-\beta)\frac{\sin\beta}{(s-\tau)^2}\left(\cot\beta - \frac{\sin\beta}{s-\tau}\right)ds\,.$$

To evaluate this integral it is convenient to put the integral (10.10) for V in a slightly different form. For $\psi = -\beta$ the integrand in the second integral of (10.10) does not have $\zeta = 0$ as a singularity. The path W' can therefore be deformed into the path W'' shown in Fig. 11, and

$$(11.5)\qquad V(\sigma,-\beta) = \frac{1}{2\pi i}\int_{W''} q_\xi\cdot\frac{\pi}{2\beta}\sec\frac{\pi\zeta}{2\beta}\,d\zeta$$

where ψ is set equal to $-\beta$ in q_ξ. Substituting from (11.5) into (11.4) we obtain (the inversion of the order of integration is easily justified)

$$(11.6)\quad M_V = -2\pi\rho a^2\cdot\frac{1}{2\pi i}\int_{W''}\left(\int_1^\infty q_\xi\cdot\frac{\sin\beta}{(s-\tau)^2}\left(\cot\beta - \frac{\sin\beta}{s-\tau}\right)ds\right)\frac{\pi}{2\beta}\sec\frac{\pi\zeta}{2\beta}\,d\zeta$$

but

$$q_\xi = \frac{a}{2}\left(2\frac{\partial}{\partial\zeta} + \cot\frac{\zeta-\beta}{2}\right)\left(\frac{s-\tau}{s-\cos\zeta}\right)^{1/2}\qquad(\zeta = \xi + \beta)$$

and so (since the inversion of the order of integration and differentiation is plainly valid)

$$\int_1^\infty q_\xi \cdot \frac{\sin\beta}{(s-\tau)^2}\left(\cot\beta - \frac{\sin\beta}{s-\tau}\right)ds = \frac{a}{2}\left(2\frac{\partial}{\partial\xi} + \cot\frac{\xi-\beta}{2}\right) f(\zeta)$$

where

$$(11.7) \qquad f(\zeta) = \int_1^\infty \left(\frac{s-\tau}{s-\cos\zeta}\right)^{1/2} \frac{\sin\beta}{(s-\tau)^2}\left(\cot\beta - \frac{\sin\beta}{s-\tau}\right)ds$$

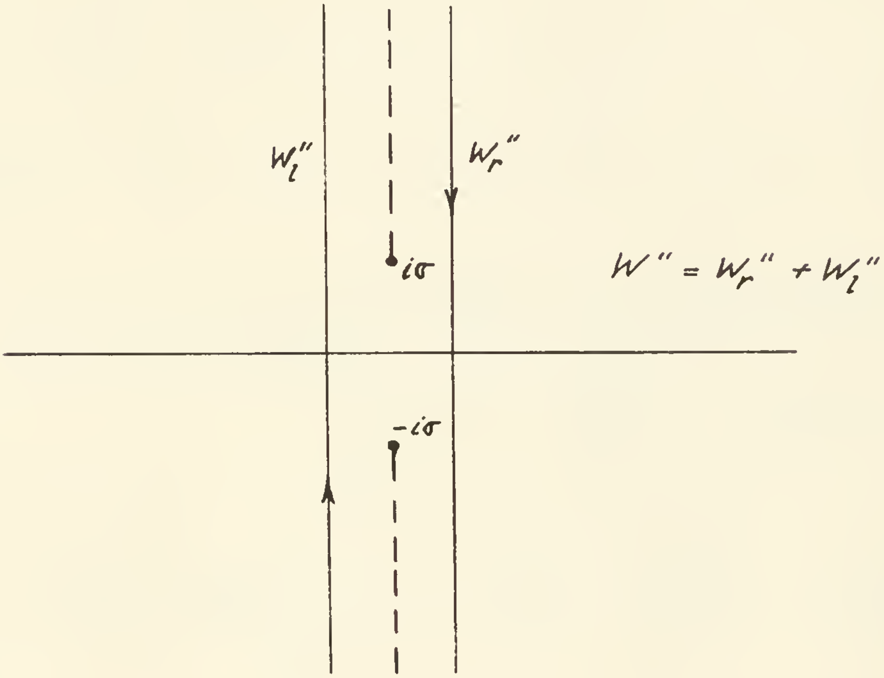

Figure 11

The integral (11.7) is easily evaluated, and consists of two parts. The first part corresponds to the integration over values s from 1 to $\cos\zeta$ and has opposite signs for ζ on opposite sides of the imaginary axis. On the other hand the second part, which corresponds to the integration from $\cos\zeta$ to ∞, is single-valued across the imaginary axis and

so contributes nothing to the integral (11.6) because W_r'' and W_ℓ'' are traversed in opposite directions. The contributions of the integration from 1 to $\cos\zeta$ is

$$\int_1^{\cos\zeta} \left(\frac{s - \tau}{s - \cos\zeta}\right)^{1/2} \frac{\sin\beta}{(s - \tau)^2}\left(\cot\beta - \frac{\sin\beta}{s - \tau}\right) \, ds$$

$$= \pm \frac{2}{3} \sin\beta \cdot \left(\frac{\partial}{\partial\beta} + \frac{3}{2}\cot\beta \right) \left[\csc\beta \cdot \left(\csc\frac{\zeta-\beta}{2} + \csc\frac{\zeta+\beta}{2}\right)\right]$$

where the plus sign is to be taken on W_r'', the minus sign on W_ℓ''. Hence

$$(11.8) \quad M_V = \frac{4}{3}\pi a^3 \rho \sin\beta \cdot \frac{1}{2\pi i}\int_{W_\ell''} \frac{\pi}{2\beta}\sec\frac{\pi\zeta}{2\beta} \cdot \left(2\frac{\partial}{\partial\zeta} + \cot\frac{\zeta-\beta}{2}\right)\left(\frac{\partial}{\partial\beta} + \frac{3}{2}\cot\beta\right) \cdot \left[\csc\beta \cdot \left(\csc\frac{\zeta-\beta}{2} + \csc\frac{\zeta+\beta}{2}\right)\right] d\zeta$$

$$= \frac{2}{3}\pi \rho a^3 \frac{1}{2\pi i}\int_{W_\ell''} \left(2\csc^3\frac{\zeta+\beta}{2} - \csc^3\frac{\zeta-\beta}{2}\right) \cdot \frac{\pi}{2\beta}\sec\frac{\pi\zeta}{2\beta} d\zeta$$

But

$$\int_{W_\ell''} \left(\csc^3\frac{\zeta+\beta}{2} + \csc^3\frac{\zeta-\beta}{2}\right) . \sec\frac{\pi\zeta}{2\beta} d\zeta = 0$$

since the integrand is an odd function of ζ. Therefore

$$(11.9) \quad M_V = - 2\pi\rho a^3 \frac{1}{2\pi i}\int_{W_\ell''} \csc^3\frac{\zeta-\beta}{2} \cdot \frac{\pi}{2\beta}\sec\frac{\pi\zeta}{2\beta} d\zeta \ .$$

Finally by making the substitution $\frac{\pi}{2\beta}(\zeta - \beta) = z$, we obtain

$$(11.10) \qquad M_V = 2\pi\rho a^3 \frac{1}{2\pi i}\int_{W_\ell'''} \csc^3 \frac{\beta z}{\pi} \cdot \csc z\,dz$$

where W''' is the path of integration shown in Fig.12. The total virtual mass M is $M_V - M_z$, where M_V is given by (11.10) and M_z by (11.3).

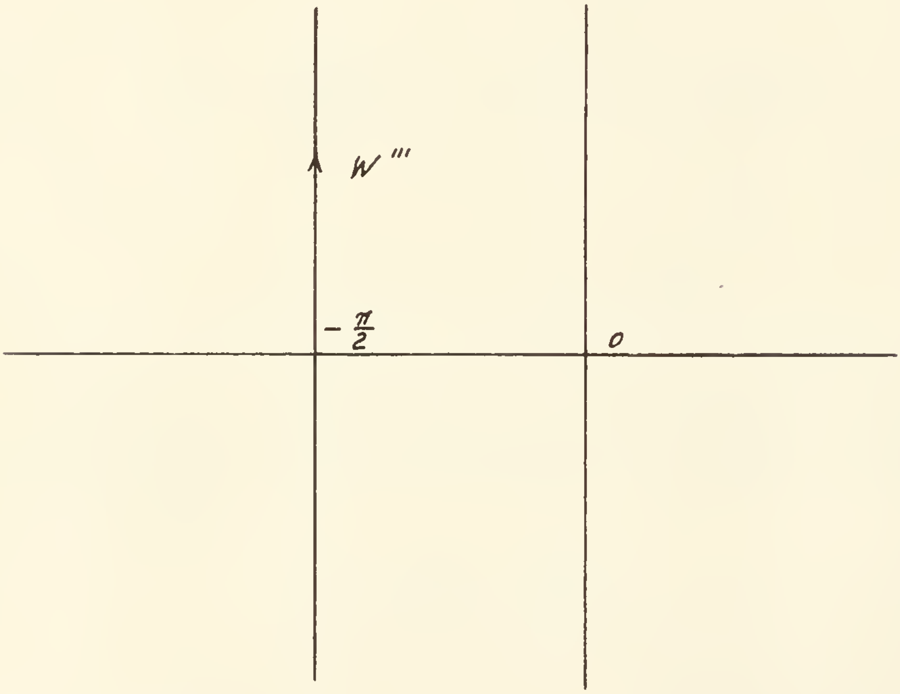

Figure 12

By (3.7) the dimensionless virtual mass is

$$m = \frac{M}{\frac{1}{2}\pi \rho A^3} .$$

Since $a = A \sin \beta$ (see Fig. 10), we have from (11.3) and (11.10)

(11.11) $$m = m_V - m_z ,$$

where

(11.12) $$m_V = 2 \frac{\sin^3\beta}{\pi i} \int_{W'''} \csc^3 \frac{\beta z}{\pi} \cdot \csc z dz$$

and

(11.13) $$m_z = \frac{2}{3}(2 + 3 \cos \beta - \cos^3\beta) .$$

To find C_p (see (3.9)) it is necessary to calculate the derivative of m with respect to $b = \frac{B}{A} = 1 + \cos \beta$ (see Fig. 10). We have

(11.14) $$\frac{\partial m}{\partial b} = \frac{\partial m_V}{\partial b} - \frac{\partial m_z}{\partial b} ,$$

where

(11.15) $$\frac{\partial m_V}{\partial b} = - 3 \cot \beta \csc \beta m_V + \frac{12 \sin^3\beta}{\pi} \cdot \frac{1}{2\pi i} \int_{W'''} z \csc^3 \frac{\beta z}{\pi} \cdot \cot \frac{\beta z}{\pi} \csc zdz$$

and

(11.16) $$\frac{\partial m_z}{\partial b} = 2 \sin^2\beta .$$

12. The virtual mass in special cases. (i) The integral (11.12) can be evaluated in terms of residues when the angle β is a rational multiple of π. Suppose that

$$\beta = \frac{n\pi}{q} \tag{12.1}$$

where n and q are relatively prime integers and $n < q$. Then (11.12) becomes

$$m_V = 4 \sin^3\beta \cdot I \tag{12.2}$$

where

$$I = \frac{1}{2\pi i} \int_{W'''} \csc^3 \frac{nz}{q} \cdot \csc z \, dz \; .$$

Let δ be a fixed positive number. Then

$$\frac{1}{2\pi i} \int_{W'''} \csc^3 \frac{nz}{q} \cdot \csc z \cdot e^{-\delta z} \, dz$$

$$= - \text{ sum of residues to the right of } W'''$$

$$= - \frac{1}{1-(-1)^{n+q} e^{-\delta q\pi}} \cdot \text{ sum of residues between } 0 \text{ and } q\pi \, .$$

Calculating the residues between 0 and $q\pi$, letting $\delta \to 0$ and observing that the coefficient of $\frac{1}{\delta}$ must vanish, we obtain

$$I = \frac{1}{2}\Bigg[\sum_{j=1}^{q-1} (-1)^{j-1} \csc^3 \frac{jn\pi}{q} + \frac{q}{2n} \sum_{k=1}^{n-1} (-1)^{k-1} \left(\csc z + \frac{q^2}{n^2} \frac{d^2}{dz^2} (\csc z) \right)_{z = \frac{kq\pi}{n}} \Bigg] \tag{12.3}$$

if $n + q$ is odd, and

$$(12.4) \quad I = \frac{1}{q\pi}\left[\left(\frac{q^3}{6n^3} + \frac{q}{2n}\right) + \pi\sum_{j=1}^{q-1}(-1)^j\, j\cdot\csc^3\frac{j\pi}{q}\right.$$

$$\left. + \frac{q}{2n}\sum_{k=1}^{n-1}(-1)^k\left[z\cdot\csc z + \frac{q^2}{n^2}\frac{d^2}{dz^2}(z\cdot\csc z)\right]_{z=\frac{kq\pi}{n}}\right]$$

if $n + q$ is even. Using these formulas a table of values for m was computed by the Mathematical Tables Project operating under the Applied Mathematics Panel. These values were used in plotting the graph of plate 1.

For the purpose of checking, it is worth while to calculate the virtual mass in certain easy special cases where it can be calculated by other means.

(ii) If $\beta = \frac{\pi}{2}$, we see from (12.2) and (12.3) (with $n = 1$, $q = 2$) that $m_V = 2$ and from (11.13) that $m_z = \frac{4}{3}$. Hence

$$m = \frac{2}{3}.$$

This trivial case corresponds to the flow about a sphere in an infinite fluid (but only half of the fluid is involved) and the virtual mass is then known to be as stated.

(iii) If we let $\beta \to 0$ we obtain from (11.12) that

$$m_V \to 4\pi^3 \cdot \frac{1}{2\pi i}\int_{W'''}\frac{\csc z\,dz}{z^3} = 4\sum_{j=1}^{\infty}\frac{(-1)^{j-1}}{j^3},$$

and from (11.13)

$$m_z \to \frac{8}{3}$$

Thus the virtual mass of the fluid when the sphere is tangent to the free surface from below ($\beta = 0$) is

$$m = 4\left[\sum_{j=1}^{\infty}\frac{(-1)^{j-1}}{j^3} - \frac{2}{3}\right] .$$

This value agrees with the limit obtained when a completely immersed sphere approaches the surface (see plate 1 and Appendix B), and so is a consequence of known formulas (see [1], page 447).

(iv) Taking $\beta = \pi$, the virtual mass is obviously zero. However if we keep a (instead of A) fixed, then we obtain the mass for a circular disc of radius a. Taking $\beta = \pi$ in (11.13) and (11.10) we obtain

$$M_V = 2\pi\rho a^3 \cdot \frac{1}{2\pi i}\int_{W'''} \csc^4 z\,dz = \frac{4}{3}\rho a^3 ,$$

$$M_z = 0 ,$$

and so $M = M_V - M_z = \frac{4}{3}\rho a^3$. This is also a known result (see [1], page 428).

13. Derivative of the virtual mass for rational β. By (11.15) it remains to evaluate only the integral

$$J = \frac{1}{2\pi i}\int_{W'''} z \csc^3\frac{\beta z}{\pi}\cot\frac{\beta z}{\pi}\csc z\,dz .$$

We suppose that $\beta = \frac{n\pi}{q}$, $(n,q) = 1$, and (as above) let δ be a fixed positive number so that

$$(13.1)\qquad \frac{1}{2\pi i}\int_{W'''} \csc^3\frac{nz}{q}\cot\frac{nz}{q}\csc z\,e^{-\delta z}dz$$

$$= -\frac{1}{1-(-1)^{n+q}e^{-\delta q\pi}}\cdot \text{sum of residues between } 0 \text{ and } q\pi .$$

Calculating the residues between 0 and $q\pi$ and equating the coefficients of δ on both sides of (13.1), we find that if $n + q$ is odd then

$$J = \frac{1}{2}\Bigg[\pi \sum_{j=1}^{q-1} (-1)^{j-1} j \csc^3 \frac{jn\pi}{q} \cot \frac{jn\pi}{q}$$

$$+ \frac{q^2}{6n^2} \sum_{k=1}^{n-1} (-1)^{k-1} \left(\frac{d}{dz}(z \csc z) + \frac{q^2}{n^2} \frac{d^3}{dz^3}(z \csc z)\right)_{z = \frac{kq\pi}{n}}\Bigg],$$

and if $n + q$ is even

$$J = \frac{1}{q\pi} C_2 - \frac{1}{2} C_1$$

where

$$C_1 = \pi \sum_{j=1}^{q-1} (-1)^{j-1} j \csc^3 \frac{jn\pi}{q} \cot \frac{jn\pi}{q}$$

$$+ \frac{q^2}{6n^2} \sum_{k=1}^{n-1} (-1)^k \left[\frac{d}{dz}(z \csc z) + \frac{q^2}{n^2} \frac{d^3}{dz^3}(z \csc z)\right]_{z = \frac{kq\pi}{n}},$$

$$C_2 = \frac{q^2}{12n^2}\left(1 + \frac{q^2}{n^2}\right) + \frac{\pi^2}{2} \sum_{j=1}^{q-1} (-1)^j j^2 \csc^3 \frac{jn\pi}{q} \cot \frac{jn\pi}{q}$$

$$+ \frac{q^2}{12n^2} \sum_{k=1}^{n-1} (-1)^k \left[\frac{d}{dz}(z^2 \csc z) + \frac{q^2}{n^2} \frac{d^3}{dz^3}(z^2 \csc z)\right]_{z = \frac{kq\pi}{n}}.$$

Using the fact that the coefficient of $\frac{1}{\delta}$ on the right side of (13.1) must vanish, we obtain the equation

$$(13.2) \qquad \sum_{j=1}^{q-1}(-1)^j \csc^3 \frac{jn\pi}{q} \cot \frac{jn\pi}{q}$$

$$+ \frac{q^2}{6n^2} \sum_{k=1}^{n-1}(-1)^k \left[\frac{d}{dz}(\csc z) + \frac{q^2}{n^2} \frac{d^3}{dz^3}(\csc z)\right]_{z = \frac{kq\pi}{n}}$$

$$= -\left(\frac{7}{360} \frac{q^4}{n^4} + \frac{q^2}{36n^2} - \frac{17}{360}\right) .$$

This equation enables us to evaluate certain of the sums. For example, if in C_1 we make the substitutions $j = q - j'$, $k = n - k'$, we see that C_1 equals the left side of (13.2) multiplied by the factor $\frac{\pi}{2}q$.

Values for $\frac{dm}{db}$ used in plotting plate 3 were computed from these formulas by the Mathematical Tables Project.

Appendix A. The Asymmetrical Lens.

14. Construction of the potential function. We construct the velocity potential of the flow around an asymmetrical lens bounded by the spherical caps $\psi = \alpha - \beta$ and $\psi = -\beta$, where β and $\alpha - \beta$ are both positive. We suppose that the lens is immersed in an infinite fluid and that it is moving downward (i.e. in the negative z-direction) with unit velocity. The symmetrical lens is obtained by taking $\alpha = 2\beta$, and this is the case which has been discussed in the main body of the paper.

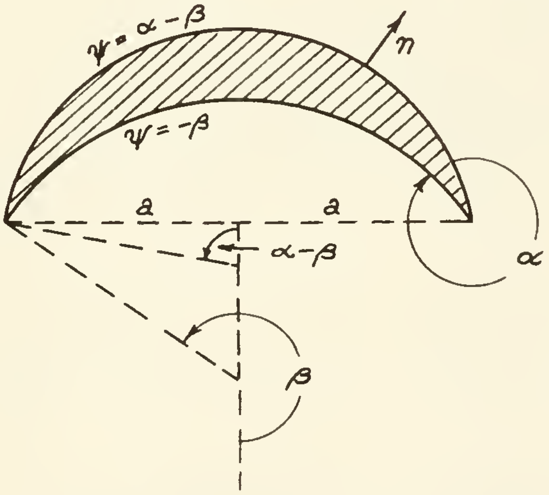

Figure 13

The desired potential function ϕ is regular at ∞ ($\sigma = 0$, $\psi = 0$) and satisfies the boundary condition

$$-\frac{\partial \Phi}{\partial n} = -\frac{\partial z}{\partial n} \tag{14.1}$$

on $\psi = \alpha - \beta$ and $\psi = -\beta$. The potential function z satisfies (14.1) but is not regular at ∞ . Set

$$V = \Phi - z \quad . \tag{14.2}$$

Then V satisfies the following conditions:

$$-\frac{\partial V}{\partial n} = 0 \quad \text{on } \psi = \alpha - \beta \text{ and } = -\beta \quad , \tag{14.3}$$

$$V \text{ behaves like } - z \text{ at } \infty . \tag{14.4}$$

In order to illustrate a remark made in section 10, namely that the n-fold Riemann space may be used if the intersection angle (here equal to α) is rational, we suppose that $\alpha = \frac{n\pi}{m}$ where n and m are relatively prime. The formulas which we obtain are then valid for all α by continuity.

The potential function

$$V(\sigma,\psi) = \sum_{k=1}^{m} \left[q^{(n)}_{2(k\alpha-\beta)}(\sigma,\psi) - q^{(n)}_{-2k\alpha}(\sigma,\psi) \right] \tag{14.5}$$

$$= \sum_{k=1}^{m} \left[q^{(n)}_{2[(k+1)\alpha-\beta]}(\sigma,\psi) - q^{(n)}_{-2k\alpha}(\sigma,\psi) \right]$$

has a vanishing normal derivative on $\psi = -\beta$ and $\psi = \alpha - \beta$ by theorem (9.1), and at ∞ ($\sigma = 0$, $\psi = 0$) all terms in the summation are bounded except $-q^{(n)}_{-2m\alpha}(\sigma,\psi) = -q^{(n)}_{-2n\pi}(\sigma,\psi) = -q^{(n)}_{o}(\sigma,\psi)$ which behaves at ∞ like $- z + o(1)$ (compare (8.5). Substituting from (8.2) into (14.5) and evaluating the sums, we obtain the formula

$$V(\sigma,\psi) = \frac{1}{2\pi i} \int_{W} q_\xi \cdot \frac{\pi}{2\alpha} \left[\cot \frac{\pi(\xi + 2\beta)}{2\alpha} - \cot \frac{\pi\xi}{2\alpha} \right] d\xi \, . \tag{14.6}$$

The desired potential function is $\Phi = V + z$.

15. Virtual mass of the fluid. The calculation of the virtual mass is similar to that of section 11. The result is

$$M = M_V - M_z \tag{15.1}$$

where

$$M_V = 2\pi a^3 \rho \sin \frac{\pi\beta}{\alpha} \cdot \left[\frac{1}{2\pi i} \int_{W_2'''} \csc^3 \frac{\alpha z}{\pi} \csc z \csc\left(z + \frac{\pi\beta}{\alpha}\right) dz - \frac{1}{2\pi i} \int_{W_1'''} \csc^3 \frac{\alpha z}{\pi} \csc z \csc\left(z - \frac{\pi\beta}{\alpha}\right) dz \right], \tag{15.2}$$

W_1''' and W_2''' being the paths shown in the diagram, and

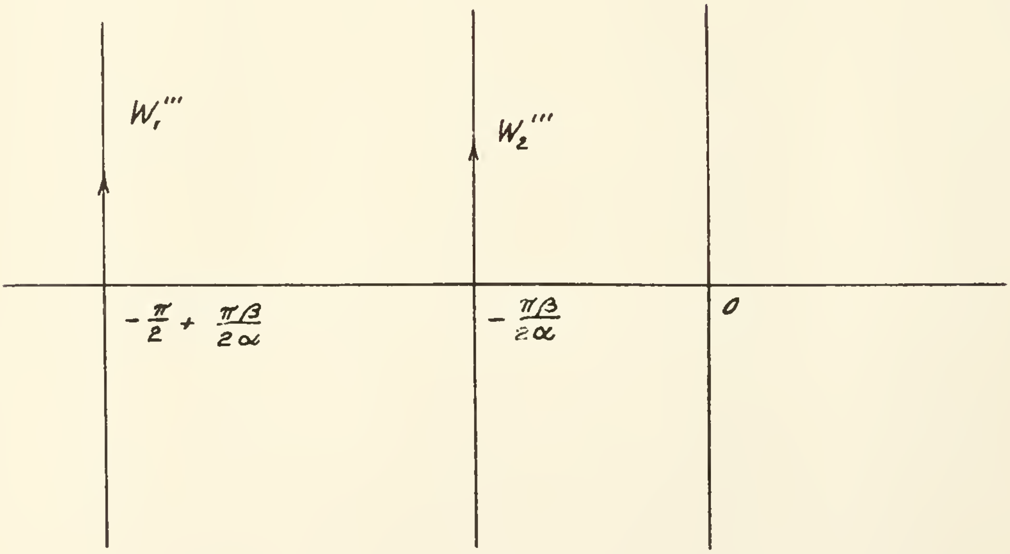
W_1'''
W_2'''
$-\frac{\pi}{2} + \frac{\pi\beta}{2\alpha}$
$-\frac{\pi\beta}{2\alpha}$
0

Figure 14

$$(15.3)\quad M_z = \frac{1}{6}\pi\rho a^3\left[\cot\frac{\beta}{2}\csc^2\frac{\beta}{2}\cdot(2-\cos\beta) + \cot\frac{\alpha-\beta}{2}\csc^2\frac{\alpha-\beta}{2}\cdot(2-\cos(\alpha-\beta))\right]$$

is the mass of the fluid displaced by the lens.

If $\alpha = 2\beta$, the virtual mass defined by (15.1) is of course twice that obtained in section 11 where only half the space was considered to be occupied by fluid.

Appendix B. The Completely Immersed Sphere.

16. Relation to the lens. We consider the case where the sphere is completely immersed. The sphere is then moving downward entirely below the surface and does not intersect it, as shown in the diagram. We shall see that the virtual mass of the fluid in this case is obtained from the formulas of section 11 by the following simple rule: (a) M_z has the

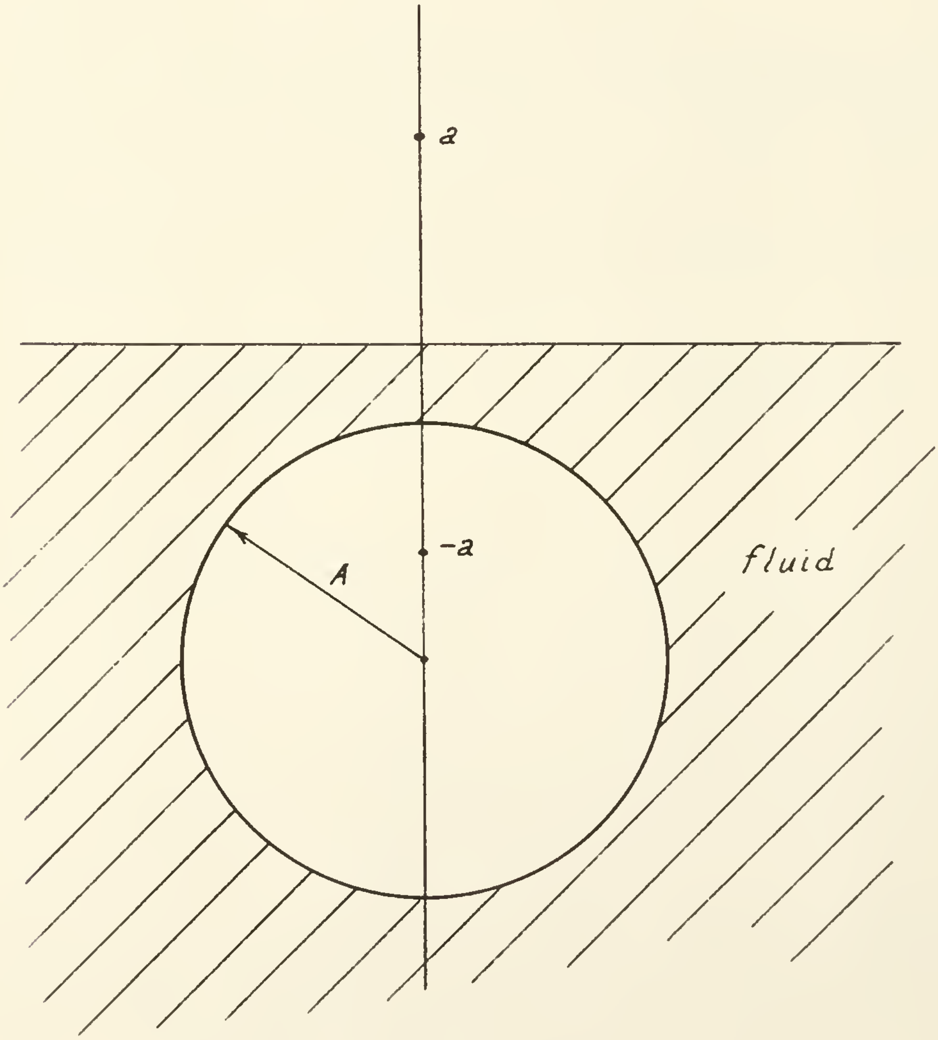

Figure 15

same meaning as before; it is the mass of fluid displaced by the sphere, therefore equal to $\frac{4}{3}\pi\rho A^3$; (b) the term M_V is obtained from the formula (11.9) merely by replacing the real quantities ζ, β and a by $i\zeta$, $i\beta$ and ia respectively.

By reflection on the plane $z = 0$, we see that the flow corresponds to that around two equal spheres moving in the line of centers with the same velocity. If the spheres are unequal, the virtual mass may be obtained from the formulas of Appendix A by the same rule. For simplicity we discuss only the symmetrical case.

17. The potential function and virtual mass of the fluid. So far σ and ψ have always been real. We now generalize by allowing them to be complex. Write $a = A \sin\beta$, where A is a fixed positive number and $-\beta$ a fixed value of ψ, and let the complex bipolar coordinates σ, ψ be connected with the complex coordinates r, z by the relations (compare (6.3))

$$r = a \frac{\sinh\sigma}{\cosh\sigma - \cos\psi} \quad , \quad z = a \frac{\sin\psi}{\cosh\sigma - \cos\psi} .$$

Let θ be real and set $x = r\cos\theta$, $y = r\sin\theta$; then x, y, z are complex cartesian coordinates in space which becomes real when σ, ψ and β are all real or all pure imaginary. In the first case σ, ψ, θ are toroidal coordinates, in the second $\operatorname{Im}\sigma$, $\operatorname{Im}\psi$, θ are the so-called bipolar coordinates in space. The locus $\psi = -\beta$ is a spherical cap in the first system and a sphere in the second; in both systems the radius is A and the center is at $r = 0$, $z = -A\cos\beta$.

The function $q_{\psi_0}(\sigma,\psi)$ defined by (7.3) remains a potential function even though σ and ψ are complex. However we are interested in this generalization only in the case where σ, ψ, ψ_0 and β are all pure imaginary, a condition we suppose

is satisfied henceforth. In order to have $r \geq 0$ we suppose also that $\sigma = i|\sigma|$ where $|\sigma| \leq \pi$.

Since σ and ψ are imaginary all the branch points of $q_\xi(\sigma, \psi)$ (as a function of ξ) lie on the line $\operatorname{Im} \xi = \operatorname{Im} \psi$. For each integer k, $k = 0, \pm 1, \pm 2, \ldots$, we cut the ξ-plane along the straight-line segment l_k connecting the two adjacent branch points $\psi - i\sigma + 2k\pi$ and $\psi + i\sigma + 2(k+1)\pi$; in the plane so cut q_ξ is single-valued. Suppose first that $|\sigma| > 0$ and let L_k denote a closed contour surrounding l_k as in the diagram. We write $W = \sum_{-\infty}^{\infty} L_k$.

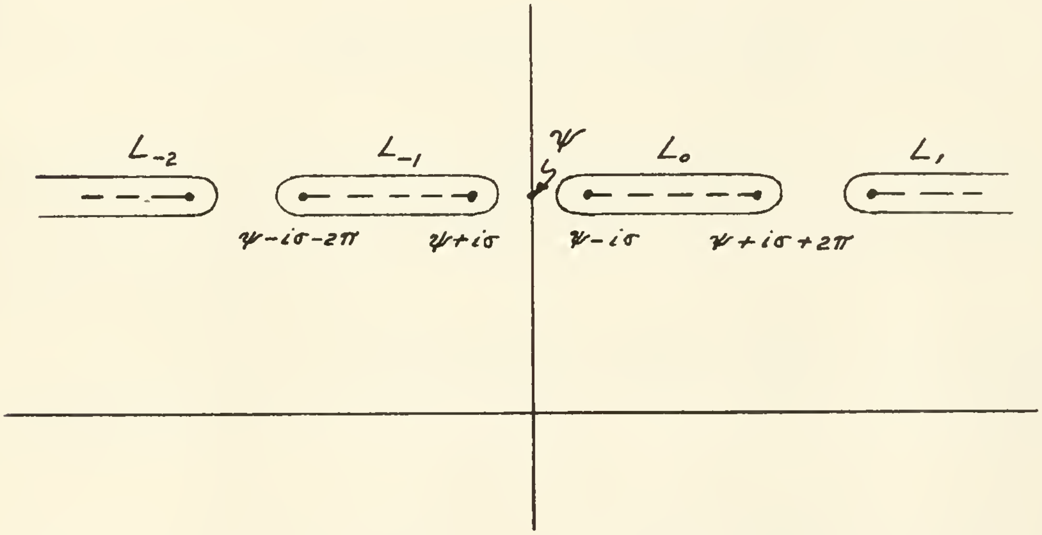

Figure 16

We suppose that the sphere is moving downward (negative z-direction) with unit velocity. Then the desired potential function Φ is regular at ∞ and satisfies the conditions that $\Phi = 0$ on $\psi = 0$ and $-\frac{\partial \Phi}{\partial n} = -\frac{\partial z}{\partial n}$ on the sphere $\psi = -\beta$. If we set $V = \Phi - z$, it is easy to verify that

$$V = -\frac{1}{2\pi i} \int_W q_\xi \cdot \frac{\pi}{2\beta} \csc \frac{\pi\xi}{2\beta} \, d\xi \quad . \tag{17.1}$$

Since β is imaginary, we observe that the integrand tends exponentially to zero as $\xi \to \infty$ on W.

The calculation of the virtual mass M of the fluid is formally similar to that of section 11. The final result is that

$$M = M_V - M_Z \tag{17.2}$$

where

$$M_Z = \frac{4}{3}\pi\rho A^3 \tag{17.3}$$

and

$$M_V = -2\pi\rho a^3 \frac{1}{2\pi i} \int \csc^3 \frac{\zeta - \beta}{2} \cdot \frac{\pi}{2\beta} \sec \frac{\pi\zeta}{2\beta}\, d\zeta , \tag{17.4}$$

the integration being along the real axis in the negative direction. Since the integration in (11.9) is along the imaginary axis in the positive direction, we obtain the rule stated in section 16.

Finally, calculating the residues in the upper half-plane we obtain for the dimensionless virtual mass $m = M/(\frac{1}{2}\pi\rho A^3)$ the formula

$$m = \frac{4}{3} + 4 \sum_{-\infty}^{\infty} (-1)^k \left[\frac{\sin\beta}{\sin(k+1)\beta} \right]^3 . \tag{17.5}$$

(Here β is of course imaginary.)

As β varies from π to 0 along the real axis and then up from 0 to $i\infty$ along the imaginary axis, the sphere passes through the surface and then moves down through the fluid to infinite depth. The virtual mass m and its derivative $\frac{dm}{db}$ vary continuously, but we see from plate 2 that $\frac{d^2m}{db^2}$ has a discontinuity at $\beta = 0$ ($b = 1 + \cos\beta = 2$).

BIBLIOGRAPHY

[1] L. M. Milne-Thomson, "Theoretical Hydrodynamics", MacMillan (1938).

[2] M. S. Plesset, "An investigation of the impact force on torpedoes entering water", Douglas Aircraft Company Report No. SM3937 (December 5, 1942).

[3] A. Sommerfeld, "Über verzweigte Potentiale im Raum", Proc. London Math. Soc. (1), vol. 28 (1897), pp. 395-429.

[4] Th. von Karman, "The impact on seaplane floats during landing", NACA Tech. Note No. 321 (1929).

[5] H. Wagner, "Über Stosz-und Gleitvorgänge an der Oberfläche von Flussigkeiten", Zeits. für ang. Math. u. Mech., vol. 12 (1932), pp. 193-215.

[6] A. M. Worthington, "A Study of Splashes", Longmans, Green and Co. (London, 1908). [Excellent photographs of the splash produced by spheres falling on a water surface.]

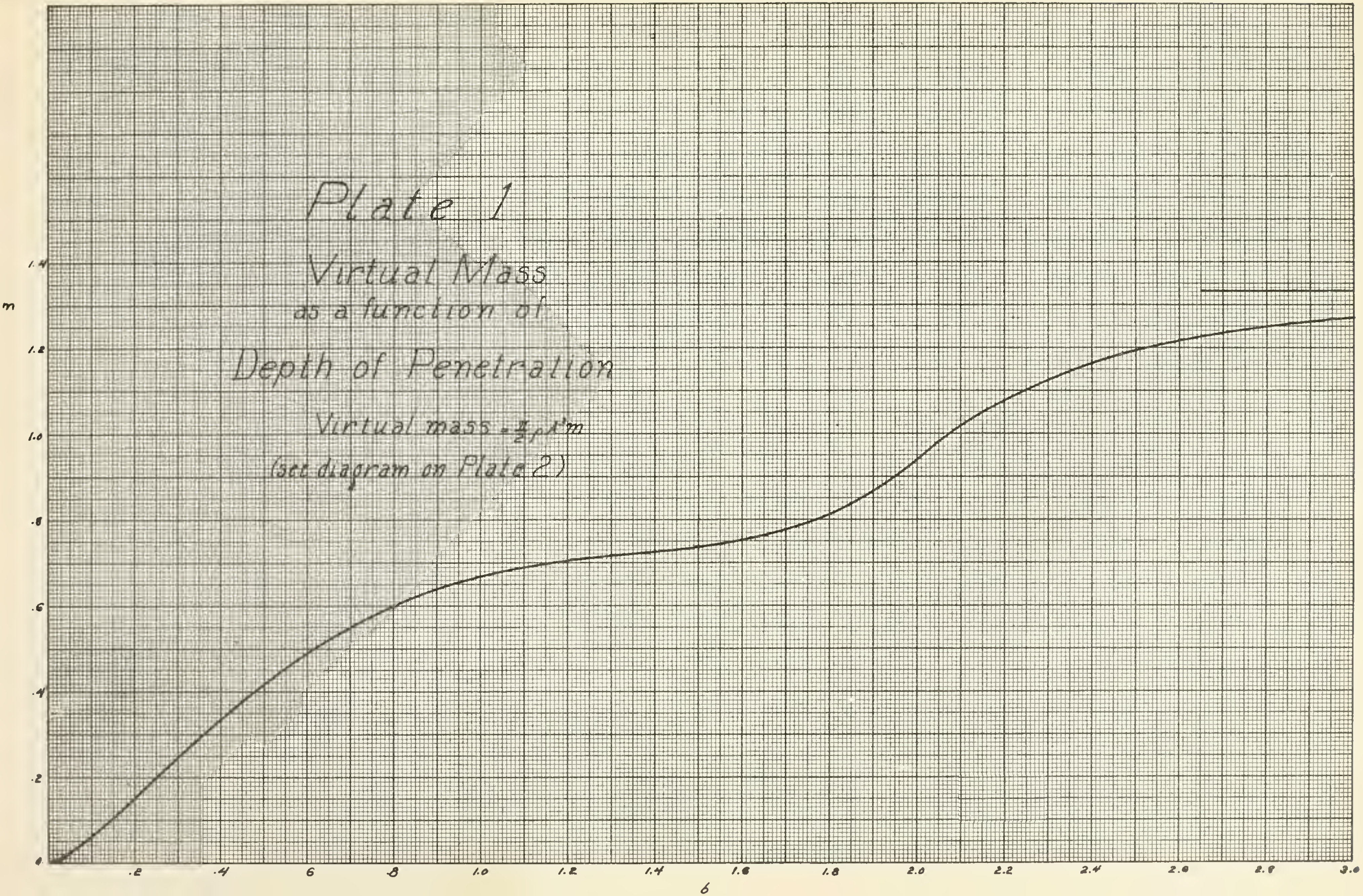

Plate 1

Virtual Mass
as a function of
Depth of Penetration

Virtual mass $= \frac{\pi}{2}\rho r^2 m$
(see diagram on Plate 2)

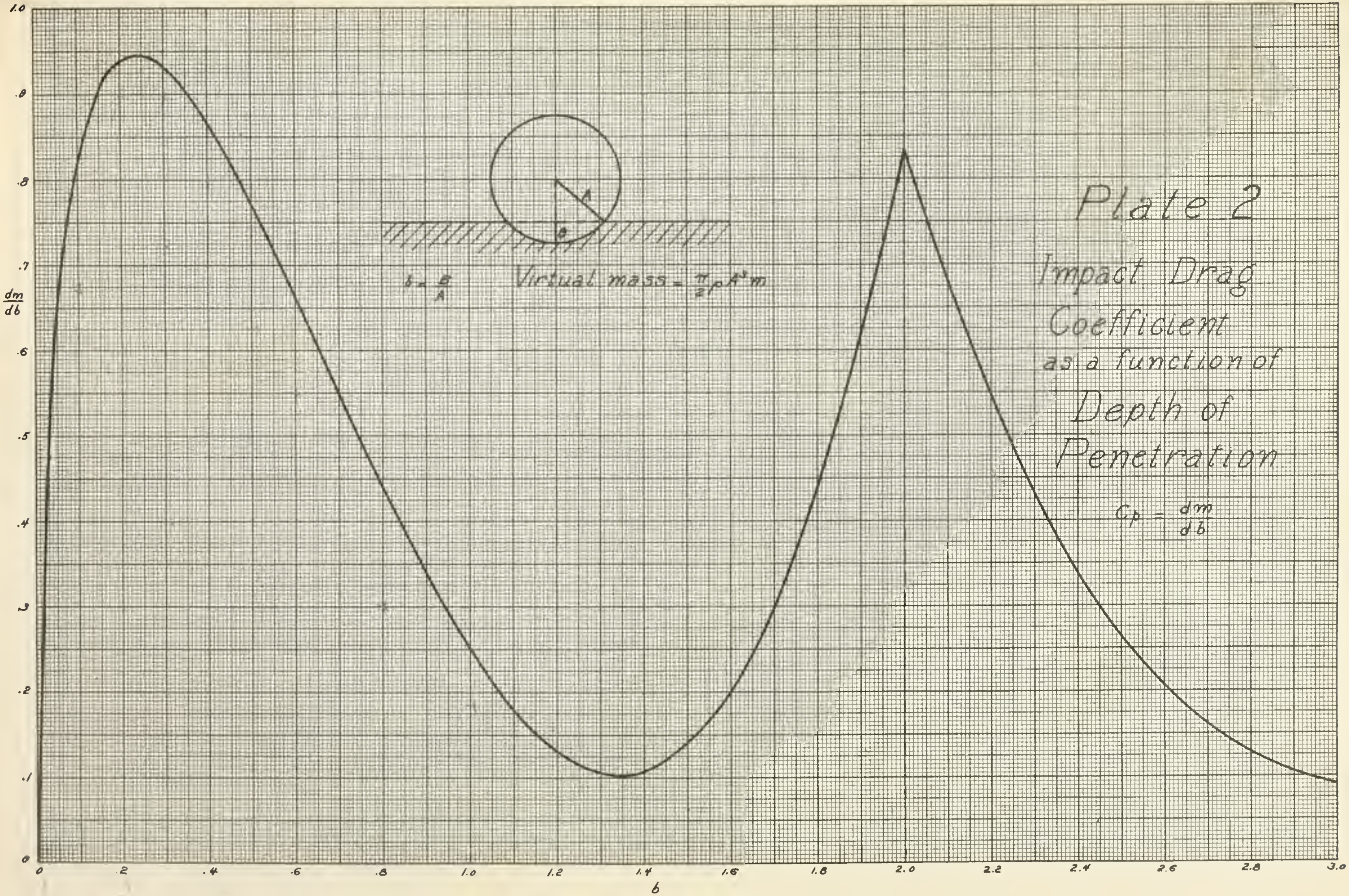Plate 2
Impact Drag Coefficient as a function of Depth of Penetration
$C_p = \frac{dm}{db}$
$b = \frac{B}{A}$
Virtual mass = $\frac{\pi}{2}\rho A^2 m$
A
B
$\frac{dm}{db}$
b
1.0
.9
.8
.7
.6
.5
.4
.3
.2
.1
0
0
.2
.4
.6
.8
1.0
1.2
1.4
1.6
1.8
2.0
2.2
2.4
2.6
2.8
3.0

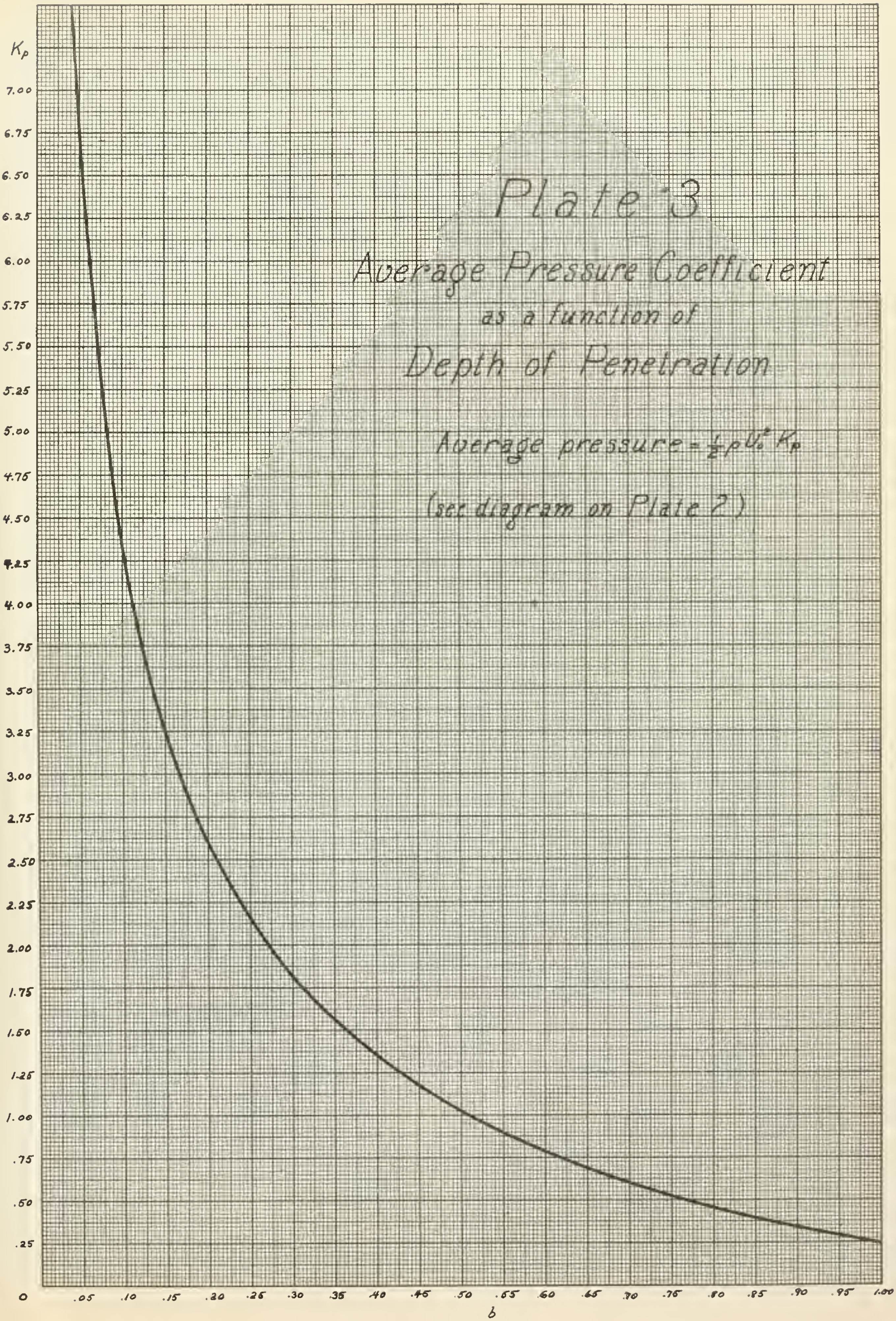

Plate 3

Average Pressure Coefficient as a function of Depth of Penetration

Average pressure $= \frac{1}{2}\rho V_0^2 K_p$

(see diagram on Plate 2)

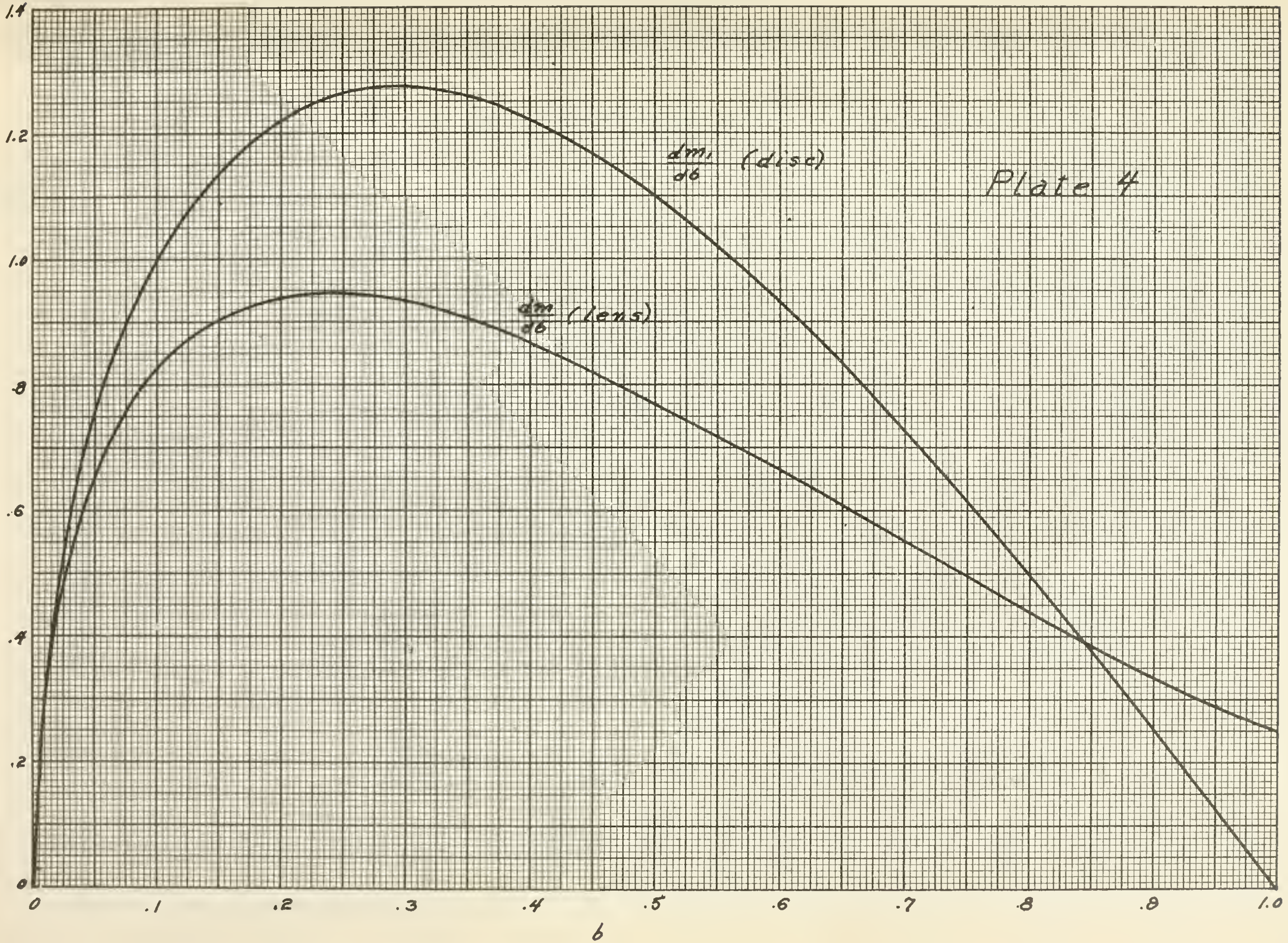

Plate 4

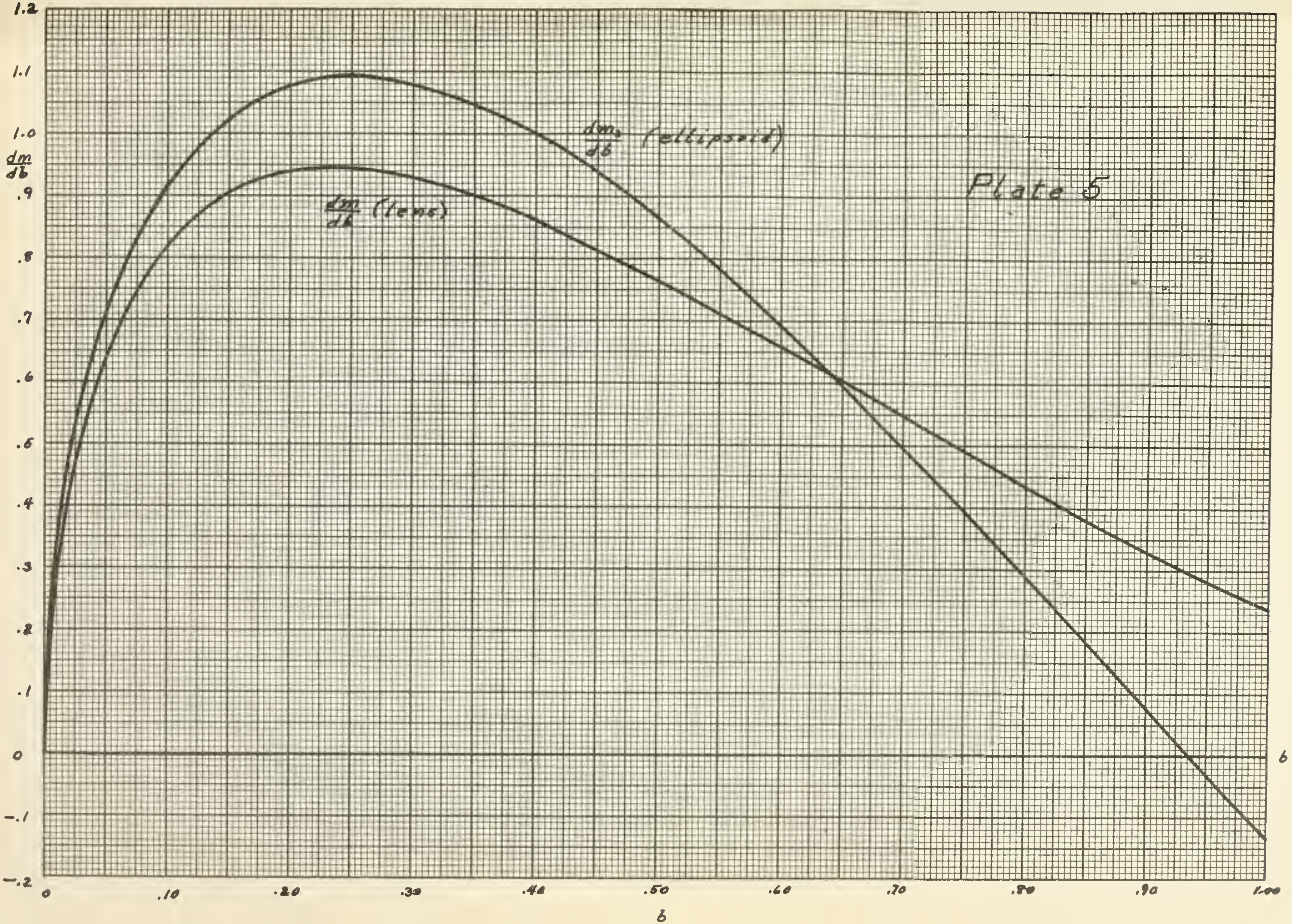
Plate 5
$\frac{dm_1}{db}$ (ellipsoid)
$\frac{dm}{db}$ (lens)
$\frac{dm}{db}$
1.2
1.1
1.0
.9
.8
.7
.6
.5
.4
.3
.2
.1
0
−.1
−.2
0
.10
.20
.30
.40
.50
.60
.70
.80
.90
1.00
b
b

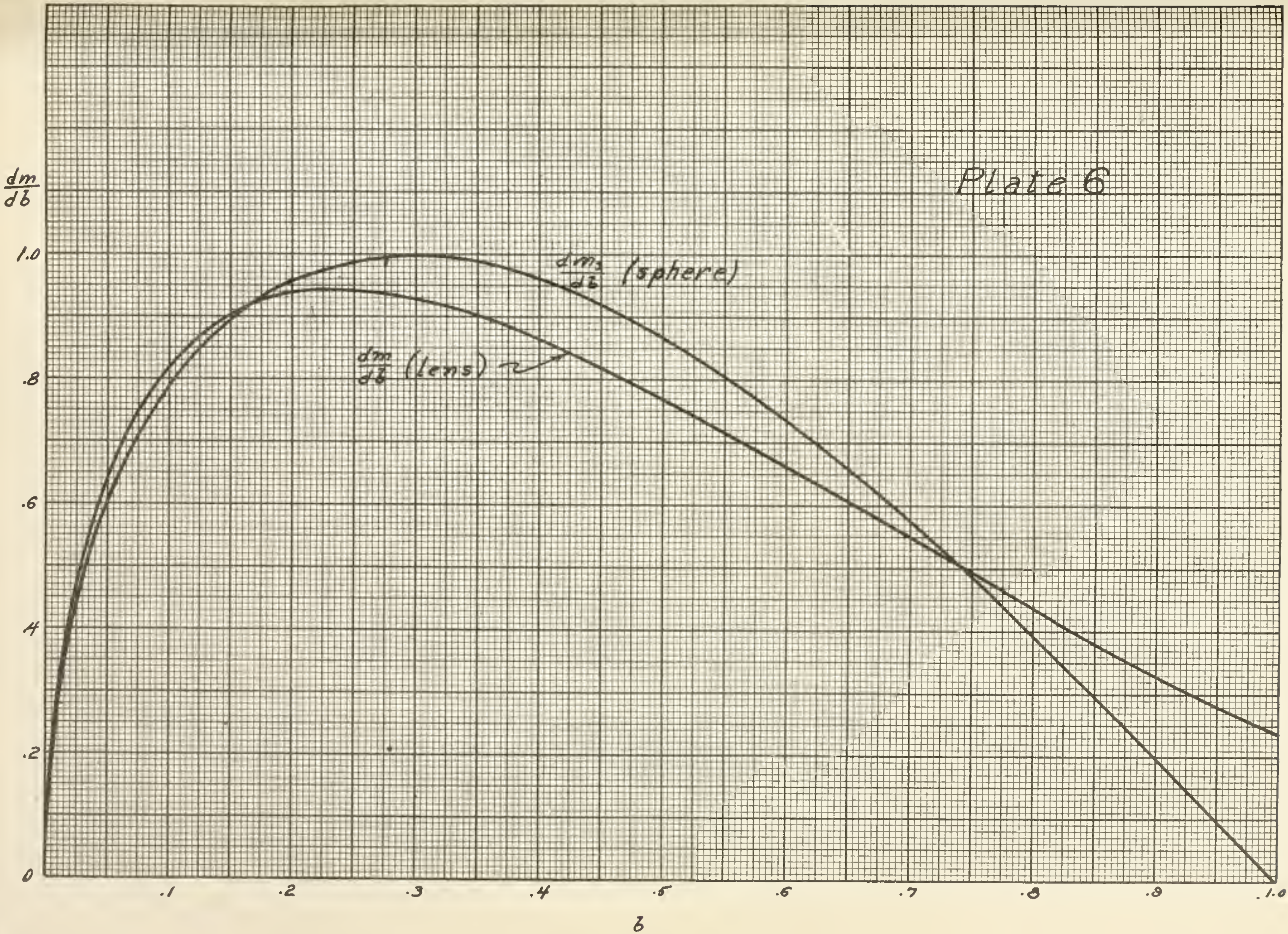
Plate 6

$\frac{dm}{db}$
1.0
.8
.6
.4
.2
0
.1
.2
.3
.4
.5
.6
.7
.8
.9
1.0
b
$\frac{dm_s}{db}$ (sphere)
$\frac{dm}{db}$ (lens)

Date Due

MAY 23 '60			
[illegible] 24 '61			
NOV 10 '67	ILL – Texas A&M		
GB	PRINTED	IN U. S. A.	

NYU
AMG-
105

c.1

Shiffman
The Force of Impact On A Sphere Striking a Water Surface.

NYU

NYU
AMG-
105

c.1

Shiffman
AUTHOR

The Force of Impact On A Sphere Striking A Water Surface.
TITLE

DATE DUE	BORROWER'S NAME	ROOM NUMBER
MAY 28	Wen Tang	
JUN 10 '50	RENEWED	
JUN 30 '50	RENEWED	

N. Y. U. Institute of
Mathematical Sciences
25 Waverly Place
New York 3, N. Y.

c.1